RSC Advances

REVIEW

View Article Online
View Journal | View Issue

Cite this: *RSC Adv.*, 2025, **15**, 18173

Metal oxide-polymer hybrid composites: a comprehensive review on synthesis and multifunctional applications

Mariam Akhtar,[a] Sehar Shahzadi,[b] Muhammad Arshad,[b] Tahreem Akhtar[c] and Muhammad Ramzan Saeed Ashraf Janjua *[b]

Received 14th March 2025
Accepted 29th April 2025

DOI: 10.1039/d5ra01821h

rsc.li/rsc-advances

A diverse family of metal oxide (MO_x)-integrated conducting polymer (CP) composites with special physicochemical properties can be used in a variety of cutting-edge technologies. This study presents a comprehensive overview of the synthesis approaches for these hybrid composites, focusing on the synergistic integration of metal oxides with CPs to enhance their structural framework as well their electrical and catalytic properties. The multifunctional applications of these materials are explored, particularly in the areas of biomedical sensing, energy retention modules, and water splitting technologies. In biomedical applications, the hybrid composites demonstrate remarkable potential for fabricating sensors with superior sensitivity and selectivity for disease diagnosis and therapeutic

[a]*School of Chemistry, University of the Punjab, Quaid-i-Azam Campus, Lahore, 54590, Pakistan*

[b]*Department of Chemistry, Government College University Faisalabad, Faisalabad 38000, Pakistan. E-mail: Dr_Janjua2010@yahoo.com; Janjua@gcuf.edu.pk; Tel: +92 300 660 4948*

[c]*Institute of Biochemistry and Biotechnology, University of Veterinary and Animal Sciences, Lahore 54000, Pakistan*

Mariam Akhtar

Mariam Akhtar is a dedicated researcher in the field of chemistry, with a strong emphasis on material synthesis, sensor development and diagnosis. Born in January 2000 in Pakistan, she completed her BS (Hons.) in Chemistry in 2018 at Government College University, Faisalabad. She completed her MS in Chemistry from the University of the Punjab Lahore Pakistan in 2024 with distinction. She conducted her research in Sensors and Diagnostic Lab, School of Chemistry ***https://aafzal.net/team/****. During her academic career, Mariam worked under the guidance of Prof. Dr M. R. S. A. Janjua, contributing impactful review articles. Her research expertise lies in advanced polymer composites doped with metal oxides and porous materials, including metal–organic framework (MOF)-derived composites. Her research holds significant potential in energy storage, catalysis, and environmental sustainability. Her passion for innovation and interdisciplinary research drives her to pursue PhD studies in polymers and sensor devices, aiming to advance cutting-edge solutions in material chemistry.*

Sehar Shahzadi

Sehar Shahzadi is an emerging researcher in the field of chemistry, with a strong focus on materials science and nanochemistry. Born in January 2001 in Pakistan, she completed her BS (Hons.) in Chemistry in 2022 and her MPhil in Inorganic Chemistry in 2024 at Government College University, Faisalabad, graduating with distinction. During her academic career, Sehar worked under the guidance of Prof. Dr M. R. S. A. Janjua, contributing to several impactful review articles. Her research expertise lies in the synthesis and characterization of advanced materials, with a particular emphasis on metal–organic framework (MOF)-derived carbon composites and nanocomposites. Her work has potential applications in energy storage, catalysis, and environmental sustainability. Motivated by a passion for innovation, Sehar is actively seeking PhD opportunities to deepen her expertise in nanochemistry and materials science.

monitoring. In the realm of energy storage, these materials exhibit enhanced charge storage capacities, improved cycling stability, and excellent performance in supercapacitors. Additionally, the catalytic properties of metal oxide-conducting polymer hybrids make them promising candidates for efficient water splitting, addressing the increasing need for sustainable energy innovations. This review highlights the current advancements, hurdles, and future directions for the advancement of these multifunctional hybrid materials.

1 Introduction

Conducting polymers (CPs) have been extensively researched over the past few decades owing to their great potential to replace their conventional inorganic counterparts. Toward the end of 1970, many scientists believed that CPs were elusive and insoluble. Numerous significant CPs have been constantly studied since Hideki Shirakawa, Alan MacDiarmid, and Alan Heeger discovered polyacetylene in 1970. They investigated that when SN_x (sulphur nitride) metal is doped with bromine, its electrical and optical properties are enhanced. Later, a study was conducted on polyacetylene, and it was found that polyacetylene doped with bromine has million times more electrical conductivity than pristine polyacetylene. This investigation was awarded the Nobel prize in 2000.[1–4] Organic CPs include polypyrrole, polyaniline, polythiophene[5] and polyacetylene, which are similar to inorganic semiconductor materials owing to their distinct electrical and optical properties. Conjugated CPs have a pattern of single and double bonds, bond polarization and conjugating electron-π dense bonds that enhance their electrical behavior. Throughout the 1970s, a range of CPs were developed; nevertheless, because of their low thermoplasticity and limited compatibility with the most conventional solvent processing of CPs and creation of soluble versions of these materials, they became a top precedence for research. Moreover, under normal conditions, CPs have limited conductivity and possess poor mechanical features, unlike most commercially available polymers. CP composites were developed to address these drawbacks.[6]

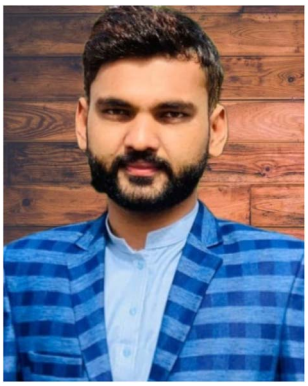

Muhammad Arshad

Muhammad Arshad, born in January 1999 in Pakistan, is a rising chemist and educationist with a strong background in inorganic chemistry. He earned his bachelor's degree in Inorganic Chemistry from Government College University, Faisalabad, in 2022. His research focuses on advanced materials, particularly MOF-derived carbon composites and nanocomposites, and he has contributed to notable publication in the field. Mr Arshad is currently working under the guidance of Dr M. R. S. A. Janjua, gaining expertise in material synthesis, characterization, and their applications in catalysis, energy storage, and environmental sustainability. Driven by a passion for innovation and discovery, he is actively seeking PhD opportunities to further his research and make meaningful contributions to the field.

Tahreem Akhtar

Tahreem Akhtar is an emerging researcher in biochemistry with a strong passion for scientific discovery and innovation. She was born in 2003, in Pakistan. She is pursuing BS (hons) in Biochemistry at the University of Veterinary and Animal Sciences, Lahore. Tahreem is currently working under the guidance of Prof. Dr M. R. S. A. Janjua, focusing on biochemical research with potential applications in health, addressing critical challenges in disease diagnostics. With a deep curiosity for molecular sciences and biochemical processes, she is dedicated to expanding her expertise through MPhil research.

Muhammad Ramzan Saeed Ashraf Janjua

Muhammad Ramzan Saeed Ashraf Janjua began his professional career as a Medical Representative at Johnson & Johnson Pharmaceuticals and Sanofi-Aventis in early 2001. While working in the pharmaceutical industry, he earned an MBA in Marketing from PIMSAT and MSc in Chemistry from the University of Sargodha, Pakistan. He was later awarded a joint PhD scholarship by the governments of China and Pakistan, completing his PhD in 2010. Dr Janjua served as an Assistant Professor at the University of Sargodha before pursuing a postdoctoral fellowship at the University of Coimbra, Portugal. He subsequently joined KFUPM, KSA, where he was promoted to the rank of full Professor in 2022. In the same year, he returned to Pakistan and joined GCUF as a Professor of Physical Chemistry, where he also serves as the Director of International Linkages.

Doping significantly increases the amount of charge carriers in CPs, which modulate and enhance the electrical properties of CPs.[7] MO_x are selected for integration in CPs because of their favorable electrical properties, eco-friendliness, cost-effectiveness, easy incorporation/doping in polymer materials, biosafety and biocompatibility.[8] MO_x@CP composites showed improved electrochemical properties: First, the quantity of metal oxide composites integrated on the electrode surface increased; (2) electron transport speed increased; (3) the distribution of metal oxide composites became more consistent; (4) the activity of electrocatalysis enhanced, and there was significant improvement in stability.

Previous studies have highlighted the excellent results in different fields achieved by MO_x@CPs. Diverse approaches exist for the monitoring of biological analytes. Some drawbacks of the traditional analytical methods are their length, the need for preliminary preparations, the need for skilled workers, and the high cost of supplies and equipment. Thus, research in the area of biosensor design has garnered a lot of attention in order to determine biomolecules quantitatively and accurately within a short period of time.[9,10] Researchers have created biosensors with a low limit of detection (LOD), great selectivity, and sensitivity using a range of CPs. These synthetic polymers have attained a great deal of interest as a suitable sustaining framework for immobilizing biological components. MO_x@CPs standout as excellent candidates for biosensors to detect biomarkers in disease diagnosis[10,11] Saddique *et al.* developed a Nb_2O_5-incorporated polythiophene biosensor for the sensing of creatinine biomarker of chronic kidney disease from saliva with a very low LOD of 34 pM and an excellent sensitivity of 4.614 $\mu A\ cm^{-2}\ nM^{-1}$.[12]

Beyond sensing application, MO_x@CPs have significant potential in energy storage devices *i.e.* in supercapacitors and batteries. Supercapacitors are widely used in automotive systems, portable electronics, and a variety of other applications. They are seen to be the best option for sophisticated energy storage systems. Because of their benefits over SCs, LIBs have been the focus of an increasing number of investigation studies.[13] When two electrodes are polarized by a neutral signal, two beds of contrasting charges arise at the boundary between the electrode and the electrolyte. The two layers are closer to one another than in traditional capacitors, having contrasting charges and being alike to an atomic gap, which results in a considerable energy gain. Because of their excessive power and energy density, SCs are therefore anticipated to lie in between Li-ion and traditional capacitors.[14] Higher efficiency, greater density of energy, and longer life cycles make SCs more required and flexible for use in electronic vehicles, portable gadgets and energy backup systems. K. P. Gautam*et al.* developed core shell NiO@PANI for supercapacitor applications. The NiO-polyaniline-based electrode material demonstrated an excellent specific capacitance of 623 $F\ g^{-1}$ at a current density of 1 Ag^{-1}. Moreover, it shows excellent stability retaining 89.4% of its initial response over 5000 cycles GCD at a current density of 20 $A\ g^{-1}$.[15] J. Yesuraj *et al.* utilized a $NiMoO_4$-PANI hybrid electrode material as a supercapacitor, which exhibited an excellent specific capacitance of 285 $F\ g^{-1}$ and remarkable stability over the 500 cycles by retaining 92% of its initial response.[16,17]

The sensible development of long-lasting, highly effective catalysts that are also cost effective and accessible is essential to electrocatalytic water splitting. Therefore, it is vital to have an effective electrocatalyst that can proficiently follow the electrolytic catalysis of the hydrogen evolution reaction (HER) and oxygen evolution reaction (OER).[18,19] MO_x@CPs stand out as excellent candidates for this purpose. Alsultan *et al.* synthesized $MnCo_2O_4$/PPy, a chemically polymerized pyrrole, with H_2O_2. They found that the hybrid substance surpassed pristine materials in the OER, with an extreme potential of about 480 mV, which is similar to the benchmark for RuO_2/C (20%). The electrocatalyst's enhanced electrical conductivity was credited with this improvement.[20]

This comprehensive review discusses various synthetic strategies, advancement, properties and applications of MO_x@CPs in different areas. Despite the substantial progress, most studies on MO_x@CPs have been limited to specific applications, often omitting the broader multifunctionality of these materials. This comprehensive study aims to bridge this gap by offering insights from various domains, including recent innovations, challenges in biomedical applications, energy storage devices, water splitting and photocatalysis, highlighting the core concepts governing their performance in each field.

1.1 Conducting polymers (CPs)

Polymers were considered to be electrical insulators before the invention of CPs such as PTh, PANI, PPy and PA,[4,21,22] as shown in Fig. 1. The significance and attention to this unique class of organic materials have increased dramatically. Among polymeric materials, CPs are regarded as the fourth generation. For many years, this class of materials have been the focus of scientific study towards energy applications because of their unique electrical conductivity, which in certain situations reached that of metals, together with their physicochemical features, which are inherited from the conventional polymeric materials.[23,24] Common polymers are easily prepared and processable, and their electrical conductivity is comparable to that of metals and inorganic semiconductors. CPs are basically synthesized macromolecules containing highly delocalized π-conjugated backbone structures and tunable side chains (Table 1).[25]

Traditional polymers such as polyethene and polyvinyl chloride comprise thousands to millions of monomer units and are stiff and soluble in various solvents. Their rigidity limits their flexibility and processability. In contrast, conjugated CPs such as PTh and PA consist of fewer monomer units and their delocalized π-electrons and alternating single and double bonds confer the flexibility and enhance their unique electrical and mechanical properties. This delocalization plays a central role in establishing polarons, bipolarons and solitons, which are unique features for their transition from insulators to semiconductors and conductors.[2]

CPs offer remarkable benefits over conventional materials, such as extensive and adjustable electrical conductivity, easy

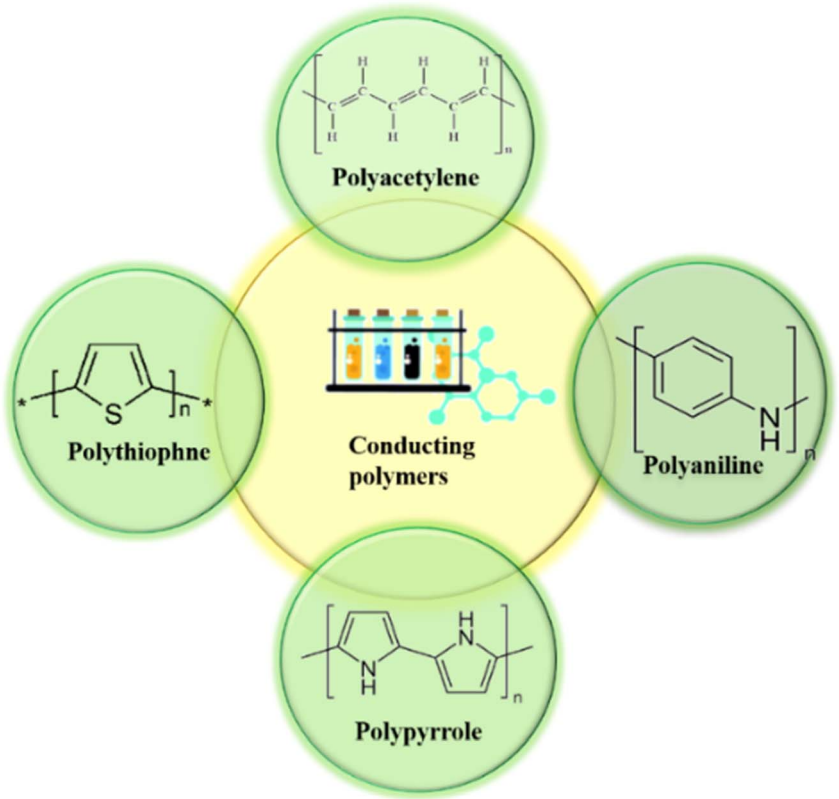

Fig. 1 Illustration of conducting polymers and their structures.

fabrication, high mechanical stability, low weight, affordability and simplicity of material production. They are appropriate for a range of applications due to their better electrochemical activity, greater surface area and electrical conductivity. The blending of CPs with additional metal oxides has produced functional nanocomposites that showed promise and succeeded in enhanced effectiveness across a variety of domains including energy harvesting sensors, energy storage devices[31] and biomedical systems.[32]

1.2 Molecular orbital theory insights into the electrical behavior of conducting polymers

1.2.1 Mechanism of conduction. Conventional theory illustrates that in CPs, delocalized electrons of π bonds are responsible for electron flow and their electrical conduction behavior. Although a single bond exclusively has a sigma bond with localized electrons, a double bond possesses both a weaker π bond and localized σ bond.[33] The displacement of π bonds, which happens in the tandem interaction bridging the first and

Table 1 Characteristics of CPs[2,4,26–29]

CPs	Properties	References
Polyacetylene-PA	Electrical conductivity 10^5 S cm^{-1}, supramolecular assemblies, doping enhanced conductivity, thermal stability	4
Polythiophene-PTh	Electrical conductivity is less than polyacetylene 400 S cm^{-1}. Thermal stability, low cost synthesis, mechanical strength and flexibility, charge transport properties	2 and 30
Polyaniline-PANI	Electrochemical properties, pseudocapacitors material, environmentally stable, ease of synthesis, good electrical conductivity 10^{-9}-10^{0} S cm^{-1}, anticorrosive properties	26 and 27
Polypyrrole-PPy	Good electrochemical capacitance, a promising candidate for energy storage devices, thermally stable, good electrical conductivity 2–100 S cm^{-1}, relatively easy to synthesize	4, 28 and 29

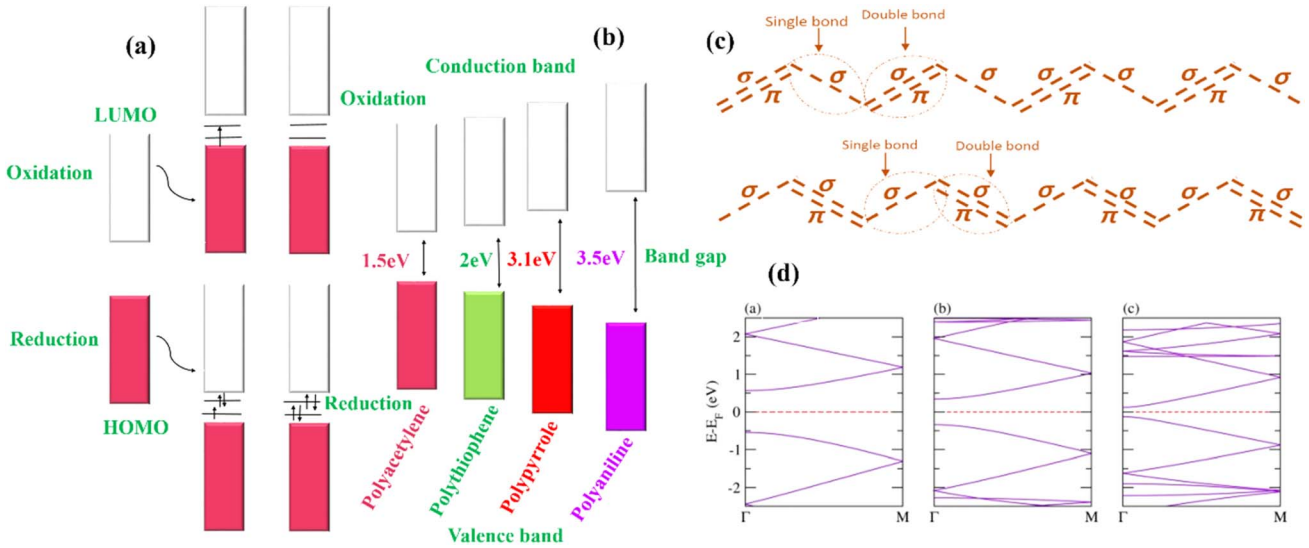

Fig. 2 (a and b) Band gap of PA, PTh, PPy and PANI to depict their conductivity and mechanism of the electrical behavior of CPs. (c) Representation of the conjugation in σ and π bonds. (d) Electronic structure of a single layer of CPs (reprinted from open-access source).[34]

second carbon atoms and the second and third carbon atoms, allows electrons to get through. Additionally, the following pair receives the π bond bridging the third and fourth carbon atoms, as shown in Fig. 2(c).[2]

MOT addresses electrical behavior at the molecular level.[2,35] In the MOT approach, molecules are considered to be a superposition of p orbitals, and this leads to a low-energy bonding molecular orbital (π) and a high-energy antibonding molecular orbital (π*). However, the highest occupied valence band HOMO and the lowest occupied conduction band LUMO are the results of combination of bonding and antibonding molecular orbitals, respectively. The band gap is the HOMO–LUMO energy gap, also known as "forbidden energy gap", "energy gap" or "fundamental energy gap".[36] In CPs, bonding and antibonding molecular orbitals create energy band with filled (π-electronic band) HOMO and vacant (π*-band) LUMO. Conjugation in the polymeric structure is increased with the increase in the number of monomer units and results in the development of wide-ranging energy states with a narrow band gap. However, electrons exhibit unrestricted motion throughout backbone starts to take place. Generally, CPs have a band gap that places them between the insulator (>3 eV) and the semiconductor within the range (0–3 eV). There are few parameters that control the conjugated polymer band gap. (1) A shift in bond length, (2) resonance energy, (3) structural planarity, (4) consequences of substituents, (5) conjugation length, and (6) donor and acceptor connections.[37] PA has a π–π* band gap of 1.5 eV and a conductivity within the range of 10^3–1.7×10^5 S cm^{-1}. PTh has a π–π* band gap of 2 eV and a conductivity in the range of 10–10^3 S cm^{-1}, whereas PPy has a band gap of 3.1 eV and a conductivity within the range of 10^2–7.5×10^3 S cm^{-1} in the same way PANI has a band gap larger than that mentioned for CPs of about 3.5 eV and a conductivity of 30–200 S cm^{-1}, as shown in Fig. 2.[2,38]

Other advanced computational approaches such as DFT provide an understanding of charge transfer in CPs. Band creation and delocalization are described by MOT, which offers conceptual basis for charge transfer in CPs. DFT enhances this image by adding electron correlation effects, charge localization and accurate band gap prediction. The Kohn–Sham approach in DFT facilitates the calculation of charge transfer properties, band structure and excitonic interactions in CPs. Hybrid functionals such as B3LYP and HSE06 are utilized to precisely access the band gaps and charge mobility, offering an extensive understanding of the electronic transport dynamic.[39]

Marcus Theory and Electron transfer mechanism describe the electron transfer as a function of reorganization energy and donor–acceptor coupling. The charge transfer k_ET depends on parameters such as Gibbs free energy change ΔG^0, electron coupling H_AB and nuclear reorganization energies (λ). Polymers with well-ordered backbone planarity and efficient π-π stacking interactions present reduced reorganization energies and, consequently, improved charge mobility and conductivity.[40]

Polaron and bipolaron transport in CPs comprises quasiparticles that emerge from structural relaxations of the polymer backbone following charge injection. The formation and stabilization of polarons and bipolarons act as crucial in charge transfer processes, improving charge flow and electrical conductivity in doped polymers. The existence of counterions incorporated during doping enhances the stability of these charge carriers, reducing coulombic interactions and improving charge carrier movement.[39,41] Modern theoretical models such as DFT, Marcus theory, and polaron/bipolaron offer insights into charge transport CPs (Table 2). By combining these theories, researchers can develop advanced next-generation CPs with enhanced electrical characteristics for applications in flexible electronic systems, biosensors and energy storage devices.

Table 2 Merits and demerits of CPs[4,25,39,42–45]

Merits of CPs	Demerits of CPs
CPs are biocompatible for sensing applications, *e.g.* disease diagnosis and tissue engineering[39]	Not all CPs are biomedically applicable as biotoxicity may arise with some biomedical applications.[39,42]
The electrical conductivity of CPs is similar to that of metals suitable for electronic applications.	Deficient specific capacitance. Less conduction than metals. They may lose stability under harsh conditions of heat and harsh chemicals[25]
They exhibit environmental and favorable cycling stability[4]	
Tunability; chemical doping is an easy way to change the properties of the material[43]	Sometimes doping can be challenging as it may deteriorate with time lead the loss of conductivity[44]
Cost effective and easily created *via* chemical and electrochemical polymerization. They are therefore commercially viable for mass manufacturing across a range of industries[45]	Large scale inexpensive chemical and electrochemical techniques may cause batch to batch variations in CPs' characteristics[4]

1.3 Properties of metal oxides

Metal oxides are a broad, versatile and attractive class of compounds due to their unique properties from metal to semiconductor and insulator. Semiconductor MO_x with narrow bandgaps have significantly grasped the place in a wide range of applications in sensors, catalysts, lithium ion electrode materials, energy storage devices and electrical devices.[46] Co_3O_4, Al_2O_3, CuO, In_2O_3, TiO_2, SnO_2, ZnO, SnO, WO_3, Fe_2O_3, and Cu_2O,CeO_2 (ref. 47) are commonly utilized in various applications (Fig. 3) because they offer excellent mechanical and chemical stability, thermal strength, and high surface area-to-volume ratios.[48]

CuO has attracted more attention in different applications than Cu_2O because of its monoclinic structure in which four oxygen atoms were bonded in a rectangular parallelogram and offer structural diversity. SnO and SnO_2 exhibit different structures, significantly rutile and tetragonal, and due to structural diversity, they have grasped a place in different applications. ZnO hexagonal wurtzite structures with intrinsic imperfections make it suitable for sensing applications. An In_2O_3 rhombohedral structure makes it a suitable candidate for good electrical properties. The unique structural features of Al_2O_3 are significantly used as the active phase in the field of catalysis. With these unique properties, MO_x stand as excellent candidates for integration into CPs.[46,49]

1.4 Doping of CPs

In doping, donor/acceptor groups are introduced into the polymer matrix. By adding or removing electrons from the CP backbone, dopant molecules are introduced, allowing for the manipulation of CP conductivity. Conjugated polymer's backbone needs to be doped with an ion or small molecule (oxidation and reduction) to enhance their properties. Charge carrier length, polymeric length and conjugation length are the parameters usually determining the doping process.[25,43] Four doping methods are briefly explained.

1.4.1 Redox p-doping. In this method, CPs are treated with Lewis acid such as chlorine and iodine which act as electron acceptors. This process involves the dopant to extract electrons from the HOMO of CPs. The electron is moved to the LUMO of dopant species, generating a hole in the polymer structure. As a result, the flow of electrons increases throughout the polymer chain to fill this hole. The overall process leads to electron mobility throughout the polymer and enhances the electrical conductivity of polymers. The conductivity of PA increased by p-type doping *trans*-$[CH(\iota)_{0.20}]_x$ and became 1.6×10^2 S cm^{-1}.[50,51]

1.4.2 Redox n-doping. CPs undergo reduction through Lewis base electron-donating species such as sodium and lithium. In this process, electrons are removed from the LUMO of doping materials and shifted to the HOMO of polymers, thereby increasing the electronic concentration in the polymer backbone, which is neutralized by dopant species counter-ions.

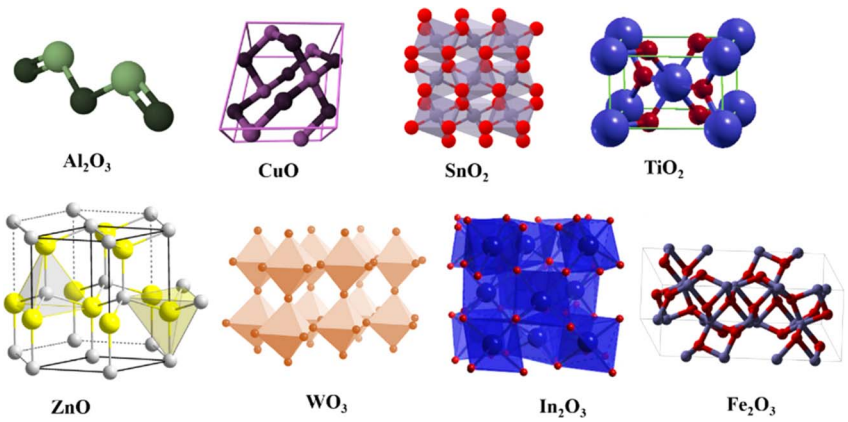

Fig. 3 Illustration of the structure of different MO_x structures: Al_2O_3, CuO, SnO_2, TiO_2, ZnO, WO_3, In_2O_3, and Fe_2O_3.

The conductivity of PA increased by N-type dopant *cis*-$[Li_{0.30}(CH)]_x$ up to 2.0×10^2 S cm^{-1}. The electrical conductivity is enhanced due to increase in the density of free charge carriers as a result of N-type doping. This doping optimized the polymeric chain and enhanced the interchain transport through an improved π–π stacking interaction, which validates the enhancement in conductivity.[51]

1.4.3 Electrochemical-p,n doping. This method of infusing the doping material is done by utilizing cathodic reduction or anodic oxidation *via* the electrolyte solution, which is a potential source of charge stabilization throughout the polymeric chain. However, the polymer backbone functions as an electron sink or an electron carrier to accomplish this procedure. The conductivity of undoped PPy is 8.77×10^{-9} S cm^{-1}, but the conductivity of the PPy/NiO dopant increased up to 4.08×10^{-7} S cm^{-1}, which is 2-fold higher than that of pristine PPy. The incorporation of dopant NiO significantly increased the electrical conductivity of PPy due to the synergetic interaction between the dopant and the CP matrix.[16,45,51]

1.4.4 Photo-induced doping. In this method, doping is carried out by high-energy radiations that transition the electrons from the valence band of low energy to the conduction band of high energy.[36,45] Charge defects are created in the polymer configuration owing to the doping process. These electrostatic flaws such as holes and electrons can serve as charge carriers. In the first step, the formation of radicals, anions/cations, *i.e.* polarons, is governed by the loss or gain of an electron from the uppermost part of the valence band or the lowest point of the conduction band. It is energetically more favorable to remove/add electrons from polarons than the other locations in the polymer backbone; as a result, there is a development of bipolarons, which is a more advantageous process than the formation of two polarons. Electrical conduction occurs in bipolarons owing to positive/negative charge's delocalization. The formation of charge imperfections in PTh is depicted in Fig. 4. Due to bipolaron bands' overlap, at high p-doping levels, the lower and higher bipolaron configurations corresponding to the occupied and unoccupied bands become energetically accessible. This opens up as a newly available valence band for electron migration, which may eventually result in a conduction mechanism that resembles a traditional metallic one.[36]

2 Synthesis of hybrid conducting polymer composites

Various methods are used to synthesize HCP composites. The most advanced and effective techniques for developing composites of CPs and a MO_x hybrid are briefly explained here. Through differential electrostatic interactions, these operations probably lead to the integration of nanounits into the primary chain of the CPs, depending on the specific MO_x and the structure of the CPs.[45]

HCPs are synthesized by the following strategies.

(1) Template-assisted polymerization

(i) Chemical polymerization

(ii) Electrochemical polymerization

(2) Sol–gel method

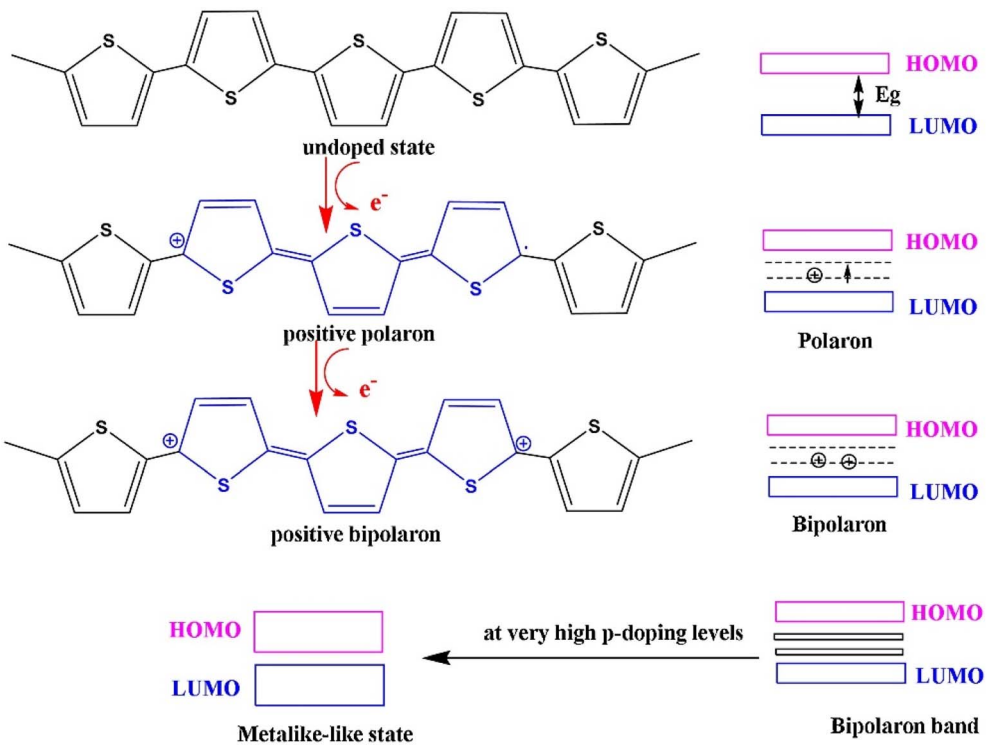

Fig. 4 Illustration of doping in polythiophene that results in the formation of polarons (reprinted from open access reference).[52]

2.1 Template-assisted polymerization

The CPs created by a template-assisted polymerization technique are highly regulated, effective and easy to synthesize. In this technique, CPs develop in predetermined forms and shapes assisted by the template.[53]

Hard templates need the CPs to be physically molded into desired shapes and rely on CPs' self-assembling activity. In the hard template approach, nanostructures are physically grown using physical templates that serve as molds or scaffolds that offer nanoscale, precise colloidal structures. The benefit of the hard template method is that the subsequent stages can employ either chemical or electrochemical polymerization. In order to synthesize a chemical template, the rigid template is immersed in a solution having an oxidizing agent, dopant, and monomer, which causes the monomer to polymerize, whether on the surface or throughout the pores or channels. The parameters of the template, monomer concentration, the type of oxidant, reaction duration, and temperature all affect the properties of the chemically produced CPs.[32]

CPs can be produced using template-directed electrochemical synthesis that uses a metal layer serving as an electrode. Charge transport during the polymerization process, the extent and time span of applied potential, and the quantity of monomers and dopants can all have an impact on the characteristics of CPs in addition to chemical considerations.[54] The most commonly employed colloidal nanoparticles are polymer microspheres or MO_x nanoparticles. The dimensions and ultimate shape of CPs are mostly governed by the colloidal nanoparticles' dimensions. This approach has multiple benefits including uniform size distribution, ease of synthesis, and large-scale acquisition. Use consistent octahedral Cu_2O crystals (0.6–1.3 μm in rhombic length) functioning as a template in a solution containing the dopant and oxidant, for instance, to create hollow octahedral PANI. The oxidative initiator can readily remove Cu_2O, which provides the new structure. Nevertheless, post-processing for template removal is time-consuming and could affect how hollow nanostructures turn up in the end.[32]

N. Shahzad *et al.* synthesized PTh by the polymerization of the monomer thiophene. A uric acid hard template was employed in oxidative template-assisted polymerization (Fig. 5). The template was removed by washing to free the cavities of the polymer.[55]

2.2 Chemical polymerization

While synthesizing HCPs, chemical polymerization is the finest method. Chemical polymerization is considered the best technique because of its quick and simple synthetic procedure.[56] It can be further divided into addition polymerization and condensation polymerization. Because chemical polymerization is inexpensive, simple to perform, and offers a variety of pathways for the production of distinct hybrid MO_x@CPs, it is widely employed.[57] In chemical polymerization, there is no need for an electrode, and it proceeds *via* oxidation of monomers in the presence of dopant ions.[58] A convenient route to create PANI is the chemical oxidation process, which includes blending the monomer of the relevant polymer with an oxidant alongside a suitable acid under ambient conditions to generate products. However, the formation of HCPs followed the same method.[1]

PTh-g-PMA/ZnO was prepared *via* chemical polymerization performed *in situ*. Its structure, morphology and properties were studied, which showed 85% enhanced luminescence properties, which make it an excellent candidate for use in photovoltaic cells. The prepared PANI/A\ZnO hybrid composites are better candidates for anti-corrosive coating, as shown in Fig. 6.[45]

A Nb_2O_5-integrated PANI sensor was created by Saddique *et al.* to detect creatinine used in *in situ* oxidative polymerization of the monomer aniline with an APS solution as an oxidative initiator ensuring the controlled growth of CPs. The synthetic

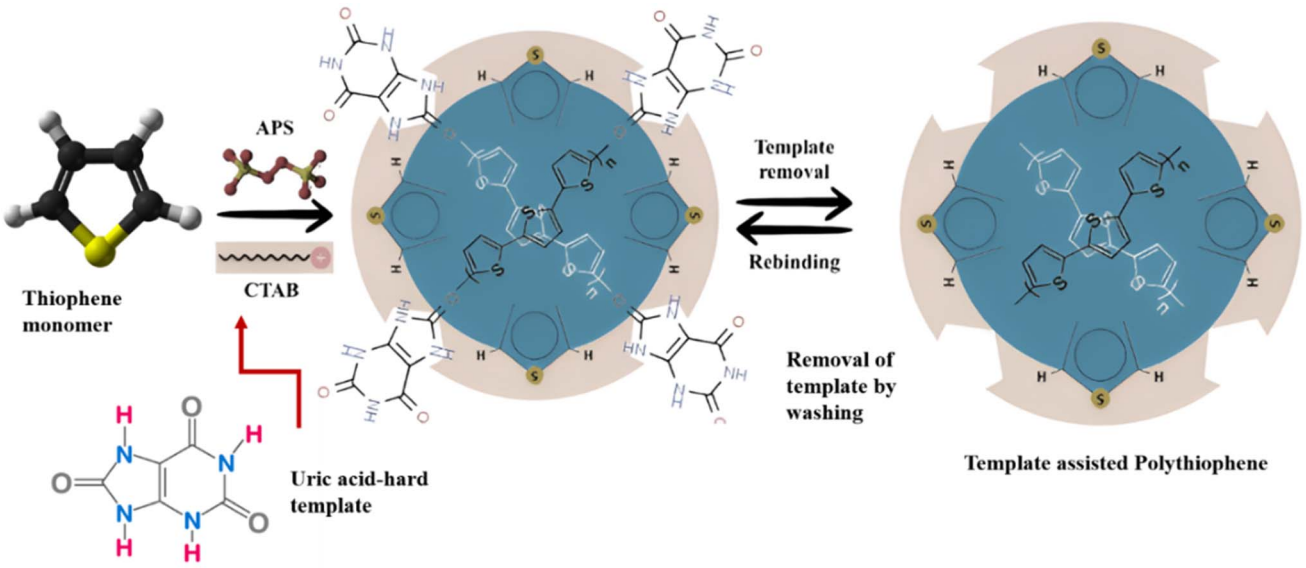

Fig. 5 Illustration of the template-assisted synthesis of polythiophene using uric acid as the hard template.

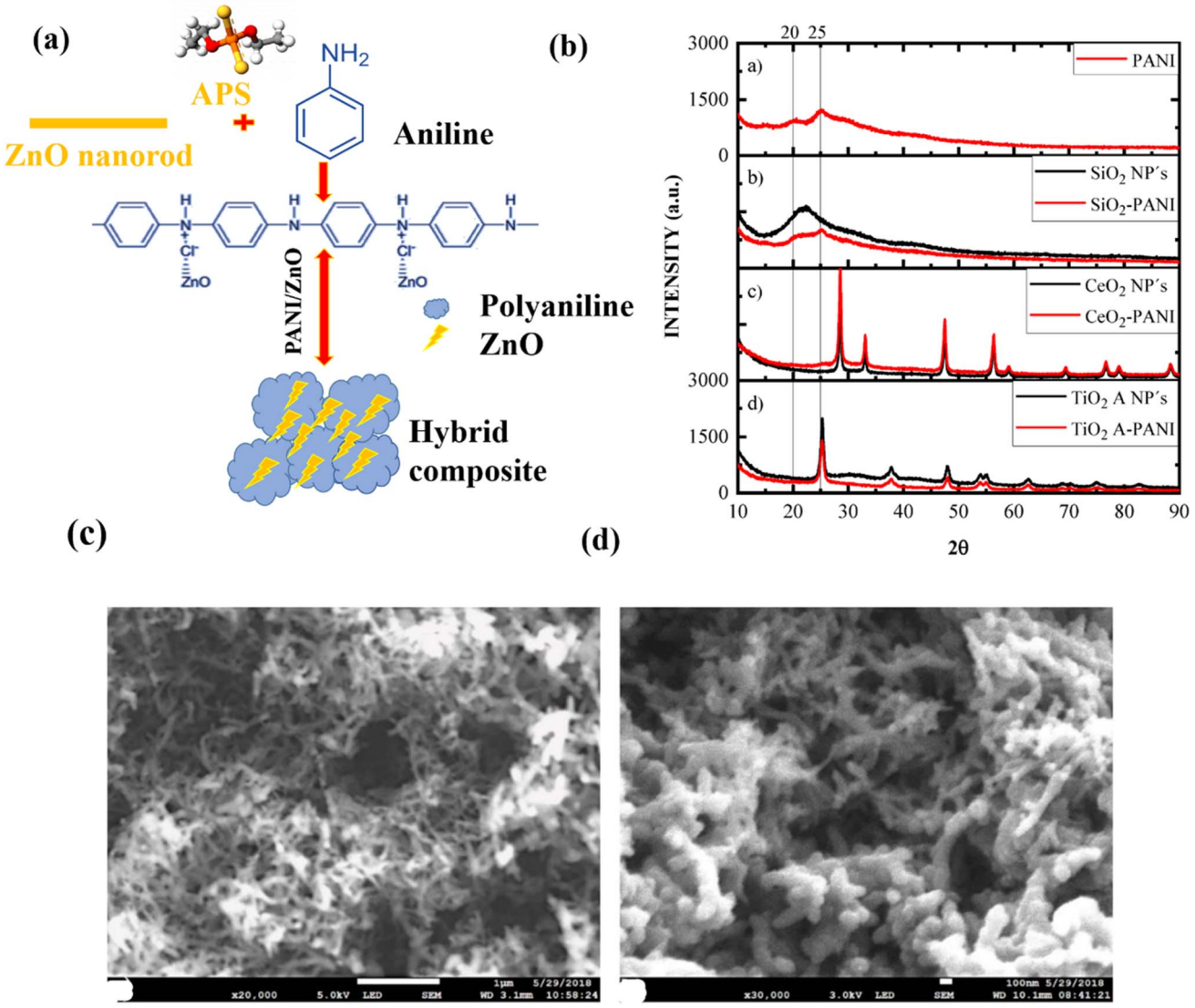

Fig. 6 (a) Synthesis of MO_x@CPs hybrid composites *via* oxidative polymerization using APS as an oxidative initiator. (b–d) XRD pattern of MO_x@PANI and SEM micrographs at 20 000 and 30 000 magnification (adapted from open source).[59]

process used diphenyl amine crosslinked aniline on the surface of Nb_2O_5,[60] as shown in Fig. 7.

2.3 Electrochemical polymerization

Electrochemical polymerization of CPs is considered non-catalytic polymerization. In electrochemical synthesis, a monomer precursor is anodically deposited on an inert metal surface, while appropriate electrolytes are analyzed. Electrochemical synthesis requires either cathodic reduction or anodic reduction of suitable electroactive functional monomers, as shown in Fig. 8. Numerous electrochemical methods such as galvanostatic charge–discharge, potentiostatic, and CV have been used for synthesis. The principal benefit of this approach is that it allows the direct coating of a polymer film onto the metal, and the coating thickness can be smoothly tuned by adjusting the electrochemical parameters.

PA was prepared by using Luttinger's catalyst, that was a combination of complex metals [VIII] containing high molecular weight and PA was produced by this catalyst. In contrast, the Ziegler–Natta catalyst utilized water-soluble solvents for catalytic processes, such as acetonitrile or water–ethanol tetrahydrofuran (THF). Nevertheless, compared to the Zeigler-Natta catalyst, it has reduced the catalytic effectiveness, and the resulting products and catalysts have nearly identical chemical and physical properties.[1]

Zhang *et al.* prepared a PPy/TiO_2 HCP using a gold substrate *via* electropolymerization and applying a steady potential of 0.85 V. The conductivity of the PPy/TiO_2 composite increased to 135 S cm^{-1}, *a* factor of ten more than that of pristine PPy (14.1 S cm^{-1}).[62] The electropolymerization process has the following advantages: in most instances, the polymer is immersed directly, capable of creating thin films. The conductivity and polymer thickness are readily manipulated.[33] It is easy to use, inexpensive, and can be completed in a solitary glass vessel, and the electrochemical preparation of CPs is a highly significant technique for thin films such as sensors.

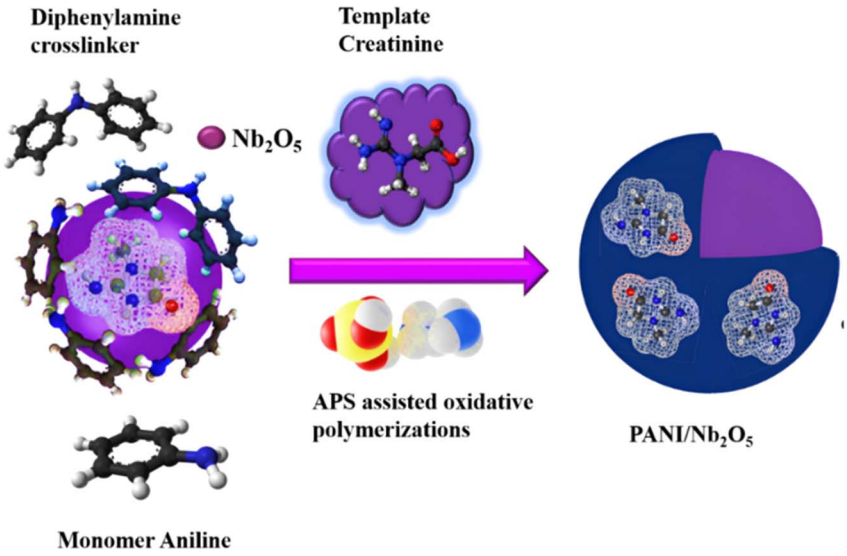

Fig. 7 Illustration of the synthesis of Nb_2O_5-integrated PANI hybrid composites *via* chemical oxidative polymerization (redrawn and modified based on information from the source).[61]

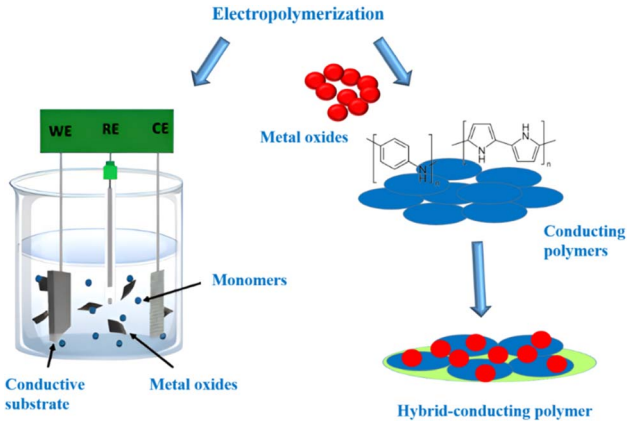

Fig. 8 Illustration of electropolymerization of HCPs in which monomers and metal oxides are included in the electrolyte in the glass vessel. Deposition of MO_x on CPs result in the formation of HCPs.

2.4 Sol–gel method

The manufacturing of HCP composites is a prospective application of flexible sol–gel technique.[63] For the first time, silicon alkoxides functioned as starting materials in the 1930s and the sol–gel process was used to create silica particles. Unlike template-assisted polymerization, the most often utilized metal alkoxides in this polymerization process are silicon alkoxide, TEOS, and TMOS (Table 3). These precursors are based on silica. Condensation and hydrolysis reactions between the organic and inorganic moieties occur simultaneously to generate HCPs. Because the Si–C bonds are durable against hydrolytic degradation, it is easier to incorporate the organic group into the inorganic framework, which is the most crucial property for the formation of HCPs. This approach has several benefits, including a low reaction temperature that makes the production of HCPs easier and improves the insertion of organic constituents into the inorganic structure conversely. By using the sol–gel method, a PANI/TiO_2 hybrid was prepared. Moreover, its morphology, structure and electrochromic characteristics were examined. The PANI/TiO_2 hybrid nanocomposite was found to exhibit improved transparency and decreased crystallinity, making it a more viable option for electrochromic devices.[45]

W. A. K. Mahmood *et al.* prepared a PANI-zirconium composite by a sol–gel technique. First, PANI was formed by dispersion polymerization of DBSA and the monomer aniline. The morphology and rod-like structure of HCPs were studied by using different techniques such as TEM, SEM and XRD. The conductive analysis of HCP composites revealed improved electrical performance, 30% more after the deposition of Zr than pure PANI.[69] The sol–gel technique for the synthesis of MO_x@CPs is presented in Fig. 9.

2.5 Photochemical polymerization

The process is less common and can be applied for the creation of some CPs. For instance, pyrrole has undergone successful polymerization into PPy using visible light irradiation, either with an appropriate electron acceptor or serving as a light sensitizer (Table 4). Horseradish peroxide is presently used to initiate the polymerization of aniline in the proximity of H_2O_2 by oxidation-radical-driven coupling reactions. It is acknowledged that aniline polymerization occurs under environmentally moderate conditions in contrast to methods involving chemicals and electrochemistry.

Several studies explored the different aspects of MO_x@CPs focusing either on the synthesis strategies or on specific applications. For instance, V. V. Tran *et al.* developed MO_x@CPs *i.e.* PPy/ZnO for CO_2 conversion, employed polymerization and sol–gel method to synthesize nanocomposites, lacking the in-depth analysis of their practical applications.[85] Silva *et al.* extensively

Table 3 Comparative analysis of template-assisted polymerization *versus* the sol–gel method[64–67]

Features	Template assisted polymerization	Sol–gel method	Ref.
Morphological control	Enable synthesis of well-defined nanostructures, but template removal is challenging	Enable control over the particle size and shape at the nanoscale but require highly precise synthetic parameters to avoid structural inhomogeneity	64 and 65
Surface area and porosity	Synthesize material with a high surface area and porosity making the material best candidate for sensing and catalytic application, but template may introduce impurities as well	High purity can be achieved, but residual solvent may require removal	57 and 68
Yield	Yield is typically high but depends on template removal efficiency	Yield varies from moderate to high and can decrease during drying	64 and 65
Cost	This method of synthesis is usually high cost due to template removal and customized material, but can be cost-effective if template is reusable	Usually cost-effective but depends on the precursor material	66 and 67
Scalability	Limited for bulk production due to template removal, suitable for nanostructure materials	Highly scalable and used industrially	64 and 65
Functionalization	Functional groups can be easily incorporated	Functionalization is not easy; limited post-synthesis	66 and 67
Mechanical strength	High mechanical integrity due to template growth	Brittle nature can lead to cracking and reduced durability	66 and 67

reviewed the role of polymeric composites in biomedical applications, as this study does not delve into the multifunctional applications such as energy storage and water splitting.[86] Ghosh *et al.* focused on CP monohybrids for fuel cell applications emphasizing their electrocatalytic properties and synthetic strategies. However, their study lacks an in-depth exploration on multifunctional applications such as biomedicine and water splitting.[87] M. Morshed *et al.* used a PANI/La_2O_3 material for supercapacitors as the PANI/La_2O_3 electrode material exhibits a higher effective capacitance of 718 F g^{-1} and a specific energy of 53.8Wh/kg. The material offers remarkable power retention over 10 000 GCD cycles.[88] Z. Hao*et al.* used core–shell PANI/WO_3 for photochemical water splitting. Hybrid material exhibits an excellent photocurrent magnitude of 0.499 mA cm^{-2}, which is 2.35 times greater than the photocurrent of bare WO_3, which is 0.212 mA cm^{-2}. The photoelectrochemical stability of the photoanode of hybrid PANI/WO_3 is increased up to 87% from 60%.[89] T. Marimuthu *et al.* used NiO-incorporated-PPy CP as a biosensor for the sensing of analyte glucose in the range of linear concentration of 0.01–0.5 mmolL^{-1} with a very

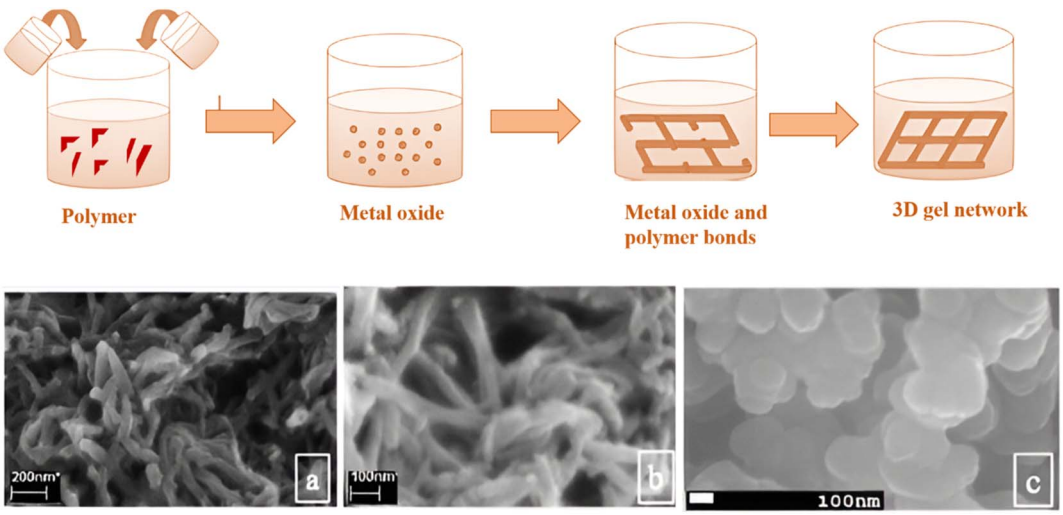

Fig. 9 (a–c) SEM micrograph of PANI nanofibers and FESEM micrographs of the diverse nanostructures of the PPy gel obtained after doping (reprinted from open source): Schematic representation of the sol–gel technique.[70]

Table 4 Different MO_x@CPs with properties, method of synthesis and applications.[45,71–76]

Hybrid conducting polymer	Conductivity	Properties/Stability	Synthetic method	Temperature	Dopant ratio	Application	Ref.
PPy/TiO_2	PPy/TiO_2 has electrical conductivity 177.69S cm^{-1} than pristine PPy 100.90S cm^{-1}	PPy/TiO_2 has good thermal stability weight loss only 15% at 200 °C	Chemical oxidation polymerization	25 °C	1 : 100	Energy storage devices	71–73
PTh/SnO_2	Conductivity of pure PTh is 5.59×10^{-4} S cm^{-1} and conductivity of PTh/SnO_2 hybrid is 9.82×10^{-3} S cm^{-1}	Excellent isothermally stable	*In situ* chemical oxidation polymerization	25 °C	1 : 7	Sensing with detection limit in ppm	77
PTh/MoO_3	PTh/MoO_3 hybrid has 18.22 times greater conductivity than pristine PTh	PTh/MoO_3 showed 1.72 times greater stability than pure PTh	*In situ* oxidative polymerization	60 °C	1 : 10	Sensing with detection limit in ppm-ppb	78 and 79
PA/ZnO	9.37 times electron mobility increased than pristine PA.	Long term stability	Sol gel method	—	1 : 10	Catalysis, photovoltaic	80
PPy/MnO_2 nanotubes	—	Good cyclic stability 88.6% over 800 cycles	*In situ* chemical deposition	160 °C for MnO_2 and 25 °C for PPy/MnO_2	—	Supercapacitor demonstrating cyclic stability 88.6% over 800 charge–discharge cycle	74 and 75
PPy/TiO_2	—	Excellent electrochemical properties having specific capacitance18.3 $mFcm^{-2}$ at 0.25$mAcm^{-2}$. 77% capacity retention rate	Electro polymerization deposition	25 °C	1 : 20	Electrochemical energy storage devices	28
PPy/SiO_2	Pristine PPy 0.88S cm^{-1} and after doping 40.4S cm^{-1}	PPy/SiO_2 much higher mechanical strength 1.7 ± 0.1 N than the normal PPy 0.2 ± 0.05 N Increased surface area and porosity	Vapor phase polymerization	25 °C	1 : 20	Sensors with detection limit 0.5 μM, catalysis	45, 81 and 82
PPy/WO_3	PPy has conductivity 7.57×10^{-9} S cm^{-1} and PPy/WO_3 has 3.77×10^{-3} six times higher than pristine PPy	Mechanical stability, pristine PPy showed exhibit 81% weight loss at 600 °C, while PPy/WO_3 showed 72% weight loss at 900 °C	*In situ* chemical polymerization	25 °C	—	Electrochemical sensors with detection limit in ppm, energy storage devices	83 and 84
PANI/TiO	—	—	*In situ* polymerization and sol gel	25 °C	2 : 1	Electrocatalyst	45 and 76

low LOD of 0.33 μmolL^{-1} with an excellent sensitivity of 1094.8 μA mmol^{-1} L cm^{-2}.[32,90] Z. Zhang *et al.* synthesized SnO_2@PPy as the anode for lithium ion batteries by employing sol–gel techniques. The synthesized component demonstrated superior dispersibility and electrochemical properties with a capacity of 932.6 mA h g^{-1} at 0.2 Ag^{-1} (100 cycles). This work provided an innovative method for dispersing MO_x@CP composites.[91] Z. Yang*et al.* developed a Fe_3O_4-integrated PPy biosensor for the sensing of glucose with the least LOD of 0.3 μM in a wide range of concentrations of 0.5 μM-34 mM with excellent stability retaining 98.1% of its response over a time period of 20 days.[92]

These studies provide comprehensive insights into MO_x@-CPs, but their scope remained confined to a single field. However their potential in other fields such as biomedical, electrocatalytic and water splitting technologies remained unexplored. Our review provides a holistic perspective that integrates synthetic strategies and implementation in real-world applications in biomedicine, energy and water splitting. By systematically analyzing these composites, this study highlights the synthetic advancements with multifunctional applications.

Hsissou *et al.* reported the synthesis and rheological characterization of a novel epoxy polymer. Their findings highlight that inorganic filler incorporation significantly increased the mechanical strength and altered the viscoelastic behavior of the polymer matrix, increasing the anticorrosive properties,[93–95] consistent with the trends observed in MO_x hybrids.[96] These findings further affirm that inorganic reinforcement in polymer matrices—whether MO_x or phosphate minerals—plays a pivotal role in improving mechanical, thermal, and viscoelastic properties through enhanced interfacial interactions and dispersion. The same group synthesized and characterized PGEPPP cured with MDA and reinforced with natural phosphate (PN). The PGEPPP/MDA/PN composite exhibited improved morphological uniformity, increased thermal stability, and modified rheological response[97,98] again consistent with the trends observed in our review. Furthermore, advanced functionalities, which are frequently overlooked in previous works, emphasize the MO_x@CP adaptability, tunability, and developing potential (Table 5). Underpinned by recent literature and state-of-the-art research, we also offer a comparative review of synthetic methodologies, comprehensive structure–property connections, and insights into the synergistic effects between inorganic and organic components.

3 Application in biomedical sensing

Sensor discipline is a device-centered technology, encompassing both fundamental and applied research, that is used in many different transdisciplinary domains.[114] Based on how they recognize the analytes of interest by sensing, sensors are often classified into two categories: (1) physical sensors and (2) chemical sensors. Nevertheless, present research endeavors are heading for the sensors using the combination of both physical and chemical features.[115] A chemical sensor serves as a tool for detecting and measuring specific analytes.[116] Its function is

Table 5 Comparison of other materials with MO_x@CPs[47,99–108] other materials

Material	Analyte	Method of detection	Linear range (μM)	LOD (μM)	Sensitivity (μA. μM^{-1})	Real sample	Ref.
Au@Fe_2O_3@rGO	Caffeic acid	Differential pulse voltammetry	19–1869	0.098	—	Coffee	99
$CoFe_2O_4$ @LSA/CT	Uric acid	Amperometric	1.9–98	0.3	0.42	Human urine	100
CuNPs-PtSPCE	Creatinine	Cyclic voltammetry	10–160	0.1	0.25	Artificial saliva	101
Nafion/Sonogel carbon	Polyphenol	Amperometric	0.042	0.06	0.099	Beer	99
Poly(N-isopropylacrylamide)	Creatinine	Cyclic voltammetry	0.5–200	0.83	0.21	Human blood	102
Cu_2O/Polyacrylic acid	Creatinine	Differential pulse voltammetry	0.1–200	6.5	—	Human urine	103
MXene/Nafion/PANI	Cholesterol	Differential pulse voltammetry	1.0×10^{-6}–1	0.149×10^{-6}	—	Human serum	104
Metal oxide enhanced CPs hybrid composites							
PANI/Fe_2O_3	Uric acid	Differential pulse voltammetry, cyclic voltammetry	0.01–5	0.038	0.433	Human urine	47
MIP-CP electrode	Creatinine	Cyclic voltammetry	0.1–100	0.05	—	Human urine	105
Cu_2O/MIP-CP	Creatinine	Differential pulse voltammetry	0–750	0.22	216	Artificial urine	106
TiO_2/PANI-AuNPs	Hydrazine	Cyclic voltammetry	0.9–1200	0.15	11.6	—	107
SnO_2/PANI	Dopamine	Differential pulse voltammetry	0.5–200	0.42	—	—	108
CuO/PCl/PPy	Glucose	Cyclic voltammetry	2–600	0.8	—	Saliva	109
Indium/Titanium oxide/PPy	Interleukin-6	Cyclic voltammetry	0.02–16	0.006	—	Human serum	110
CeO/PANI	HRS	Cyclic voltammetry	0.05–5	0.05	0.159	—	111
TiO_2/PANI	Transferrin	Fluorescence	0.00137–1.96	0.00137	—	Human serum	112
TiO_2/PANI	Glucose	Cyclic voltammetry, amperometric	20–140	5	163.14	—	113

based on the idea of target species and sensor interaction.[115,117] Leveraging bio-molecules of interest, the sensors quantify molecules of biological importance.[118] Due to the overlap in sensing techniques, sensors are deemed as a component of chemical sensors. Chemical sensors using innovative methods can identify analytes with intricate chemical structures.[116] Electrochemical sensors are acclaimed for their remarkable selectivity, accuracy and precision and are classified into amperometric sensors, impedance sensors and potentiometric sensors.[119] For more quick and selective determination of analytes, electrochemical sensors are crucial. Comparing these sensors to their spectroscopic and chromatographic parallels, they are far more affordable. It can also be adjusted to fit certain uses. For potentiometric sensors, ion-responsive electrodes are pivotal for analyte detection.[120]

A current signal is produced when the reactant is reduced or oxidized at a constant applied voltage. Amperometric biosensors measure this current signal. These sensors' ability to work is affected by multiple circumstances. The primary factor among them is the transmission of electrons between the catalytic molecule and the electrode/CP surface. Among other sensors, amperometric biosensors are frequently employed. The current signal is measured using an electrochemical method that is incredibly sensitive.[121,122]

Potentiometric biosensor is less commonly employed in sensing. When it comes to the PPy/electrode with mounted glucose oxidase, researchers have shown its advantages over amperometric biosensors. When the sensor functioned for the detection of dopamine, it showed good detectability and selectivity. The analytical signal is thought to be the potential change rate.[123,124]

Impedimetric biosensors compared to both amperometric and potentiometric sensors are infrequently employed. In order to function, impedimetric biosensors must be able to measure changes in the CP substrate's conductivity between two electrodes. The conductive nature of the component changes when the redox level or pH balance of the CP matrix changes. This sensing method takes a lot of time.[125,126] D. Minta *et al.*, fabricated an electrochemical sensor based on a ternary PANI/Fe_2O_3–SnO_2 composite on a glassy carbon electrode for the sensitive detection of dopamine and uric acid (UA).[127] The fabricated sensor demonstrated outstanding performance in detecting the target analyte, achieving an exceptionally low detection limit for UA 6.4 μM in 1.6 μM UA concentration and for DA 0.15 μM in concentration 0.076 μM at peak potential 180 mV. The sensor demonstrated excellent stability by retaining 90% of its response after use over a time period of 30 days.

3.1 In disease diagnosis – biomarker detection

3.1.1 Uric acid. UA is present in physiological fluids such as urine, saliva and serum. Serum and urine contain UA within the range of 300–500 μM and 1400–4400 μM, respectively. The elevated level of UA causes different diseases including gout, arthritis, high cholesterol, renal lesions and metabolic syndromes including heart attack and high blood pressure. Parkinson's disease and multiple sclerosis are caused by abnormally low levels of UA.[128] Many analytical methods such as HPLC, chemiluminescence, chromatography, and colorimetry are used for the detection of UA level. These conventional techniques, however, are typically laborious, complex, and instrument-expensive. The electrochemical methodology offers numerous advantages over traditional approaches including high sensitivity, minimal expense for upkeep, and rapid operation.[129,130]

S. K. Ponnaiah *et al.*[130] employed a Ag–Fe_2O_3@PANI-modified electrode for the detection of UA. The built sensor is highly responsive to the targeted analyte UA with a sensitivity of 128.29 $mAmM^{-1}$ and a remarkably low limit of detection of 102 pM. It has been proficiently accomplished to determine the UA concentration in serum and urine specimens by using the electrochemical approach. The benefits include good selectivity, a wide detection range, and quick detection. The current electrochemical sensor possesses the inherent ability to rapidly and quantitatively detect UA in real samples of patients belonging to different age groups. The sensor's selectivity was determined with different interfering analytes such as sucrose, glucose, formic acid, ascorbic acid and dopamine, which exhibited excellent selectivity by showing more response for targeted UA. On this modified electrode system, the π–π coupling connection between the analyte and the fabricated electrode active region may weaken other biological interferences while accelerating electron transport. Very low detection limits, excellent stability, and extremely high selectivity and sensitivity are all displayed by the sensor that was developed using this nanocomposite.

The Ag/Fe_2O_3@PANI-based UA sensor holds great promise for various applications, including evaluating the content of UA in human serum and urine samples, given its outstanding performance. This technique can be effectively used for the design of sensing devices, which offer a useful solution for medical diagnosis.[130]

3.1.2 Creatinine. Chronic kidney disease, a progressive acute medical condition of the kidneys, increased the mortality rate up to 41% from 1990 to 2017 in individuals of all age groups. CKD is responsible for worldwide 1.2 million fatalities per year and decreased kidney function accounts for an additional 1.4 million deaths.[131–133] The rate of kidney dysfunction has increased in the preceding fifteen years. In the event of progressive renal failure, the glomerular filtration rate decreases to less than 15 mL min^{-1}, giving rise to the retention of metabolic residues, *e.g.* urea and creatinine, as well as unbalanced serum electrolytes. In healthy individuals, the normal range of creatinine in blood is 45–140 μM per day.[134] Creatinine (Cre) is a vital biomarker for the identification of CKD and other renal disorders since it is elevated in bodily fluids such as saliva, serum, and urine.[135]

Saddique *et al.*[60] synthesized a Cre-imprinted Nb_2O_5/PANI nanostructure for the electrochemical sensing of Cre in human saliva. Cyclic voltammetry (CV), differential pulse voltammetry (DPV) and electrochemical impedance spectroscopy (EIS) confirmed that the sensor manifests exceptional sensitivity and selectivity for Cre, and improved electron transfer kinetics as compared to pristine non-imprinted PANI. The fabricated

Nb_2O_5/PANI electrode exhibits a superior sensing capacity of 3.68 μA μM^{-1} within the linear range of 0–1000 nM remarkably with a very low limit of detection (LOD) of 127 pM and an LOQ of 385 pM. The sensor exhibits excellent selectivity for the biomarker Cre over the common salivary analytes such as glucose, spermine, urea and UA, and ascorbic acid. The sensor showed excellent resilience by retaining 85% of its first reaction over a period of 5 days. Additionally, the designed sensors were evaluated with human saliva samples that are either pure or spiked with different amounts of Cre, with a recovery rate of 97.4 ± 2.83(%).

3.1.3 Spermine. Spermine is a potential biomarker of cancers such as breast cancer due to the abnormal growth of cells, as the level of polyamine is increased in physiological fluids such as saliva. The level of polyamines such as spermine and spermidine in the saliva of cancer patients is 15–20 folds upregulated. Therefore, a POC diagnostics tool is required for onsite and rapid detection of breast cancer. A budget-friendly, sensitive, and portable device was developed for non-invasive diagnosis of breast cancer using saliva.

I. Zaman*et al.* developed a $FeFe_2O_4$/PPy-based sensor for electrocatalytic oxidation and spermine monitoring in a complex mixture solution of human saliva. Molecular imprinting was employed to make this material selective and sensitive for the targeted analyte spermine. After washing, the cavities were freed to remove any trapped spermine molecule. The sensor exhibited an excellent sensitivity of 0.424 μA nM^{-1} over a linear spermine concentration range of 0–1000 nM with a very low limit of detection of 220 pM and an LOQ of 667 pM. The sensors demonstrated high selectivity towards spermine compared to other interfering salivary analytes such as guanine, tyrosine, glucose, and ascorbic acid. A stability test at alternate days over a time period of 8 days indicated that the sensor retained 80% of its initial response, which indicated the robust nature of the sensor. The sensor showed 87% response in spiked human saliva samples. Overall, the fabricated device exhibited excellent sensor characteristics. All these figures of merits of $FeFe_2O_4$/PPy confirmed that the sensors showed excellent sensitivity and selectivity only towards the targeted biomarker spermine compared to other polyamines.[136]

3.1.4 Glucose. Among the biggest hazards to health initiatives of the 21st century, diabetes mellitus (DM) is alarming.[137] DM is caused by abnormalities in insulin production, and it leads to various diseases such as neuropathy, nephropathy, skin disorders, risk of cardiovascular diseases and dementia.[113] According to WHO predictions, DM and its consequences will claim the lives of over four million adults in 2019, one death every eight seconds.[138] In 2021, there were about 537 individuals with DM. It is anticipated that there will be 643 million DM patients worldwide by 2030.[139] In the past ten years, there were observed remarkable accomplishments in the development of biosensors for potential biomarkers that are crucial for the early identification of prediabetes. Finally, we propose important biomarkers that should be taken into account as possible targets for creating extremely sensitive biological glucose sensors.[140]

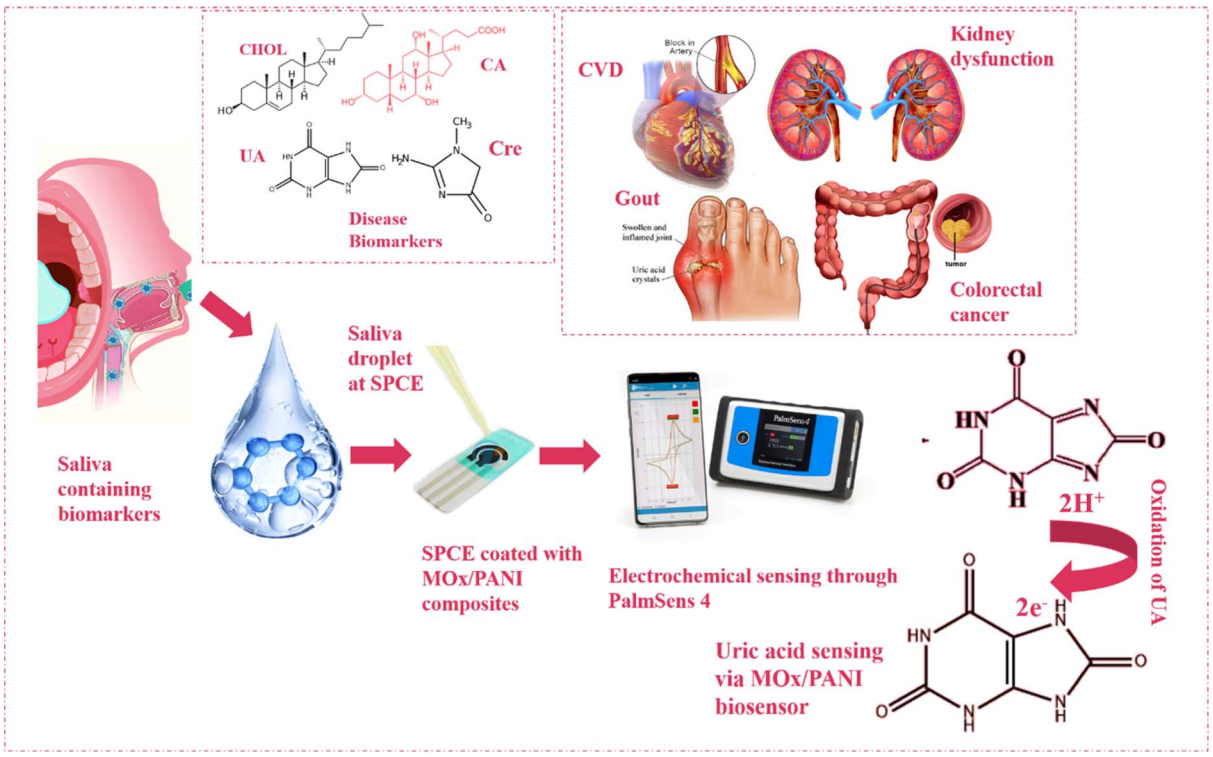

Fig. 10 Illustration of different disease biomarkers: cholesterol (CHOL), cholic acid (CA), uric acid (UA) and creatinine (Cre). Biosensing of biomarkers of diseases using an MO_x@CP-coated screen-printed electrode and electrochemical sensing through PalmSen4.

C. Karaman*et al.* developed a Ti–Nb_2O_5@PPy biosensor for the detection of a glucose biomarker of chronic diabetes. The sensor has an excellent sensitivity of 18.93 μA μM^{-1} for glucose with a very low limit of detection of 1 μM and an LOQ of 10 μM. A lot of benefits are offered by the biosensor, including its fast processing, high selectivity, and ease of use. Furthermore, a highly selective glucose detection method without any interference in plasma samples was achieved, yielding sensitivity and a detection range of 1.0×10^{-6} M. Electrochemical techniques such as CV and DPV were performed to access the effectiveness of the sensor. Thus, a new avenue for the assessing of glucose concentration in plasma specimen is made possible by the creation of an enzyme-free glucose sensor rooted on MIPs. As a result, this framework promotes the formulation and exploitation of sensors for glucose in practical applications (Fig. 10).[141]

4 Electrochemical applications

4.1 Supercapacitors

Promising technologies such as SCs have attracted some commercial significance in recent decades owing to their potential to significantly impact the market for certain industry-based devices such as smartwatches.[142–144] There are four primary types of SCs that can be distinguished based on how they store charge, namely pseudo-capacitors (PCs), hybrid SCs, asymmetric SCs (ASCs) and electric double-layer capacitors, as illustrated in Fig. 11. One of the most significant types of SCs, EDLCs, operate by a non-faradic mechanism, as shown in Fig. 12. Charge buildup appears at the electrode–electrolyte interface of this SC. Graphene and carbon nanotubes, two high-surface-area C-derived constituents, are frequently utilized as electrode materials in EDLC SCs.[145] The second most popular type of SC, known as PC, shown in Fig. 12, operates *via* a faradaic process. Redox reactions or intercalation processes are the basis for charge storage in this type of SC. PCs have demonstrated their significant potential to increase power and energy densities when compared to EDLCs.[146]

The enhanced redox activity of CPs makes them the most popular electrode material for transition MO_x such as Mn_3O_4 and for PCs.[148] A hybrid supercapacitor (SC), as illustrated in Fig. 13, combines the advantages of both electric double-layer capacitors (EDLCs) and pseudocapacitors (PCs), offering suitable energy and power densities from the PCs along with high cycling stability and reasonable specific capacitance from the EDLCs.[149,150]

Because ASCs offer a broader voltage window than symmetric SCs, they might be considered the third common SC.[151] As such, they have garnered significant attention globally. ASCs have shown both higher energy/power density and greater performance than traditional types of symmetric SCs.[14]

Electrolyte is a significant component of electrochemical SCs. They have an electrolyte, two foil electrodes, and a foil separator. SCs and electrolytic capacitors are structurally similar.[152] The separator is placed in between the electrodes after the foil has been rolled into a shape, most frequently cylindrical or rectangular. When the electrolyte is added and sealed, the bent structure is put inside a housing.[153] Unlike traditional electrolytic capacitors, the electrodes and electrolytes utilized in the production of SCs are different. Using porous materials as separators, a SC stores electrical charge and ions at the nuclear level in the holes.[116] An electrolyte is also utilized to connect the two electrodes. Aqueous, chemical, and

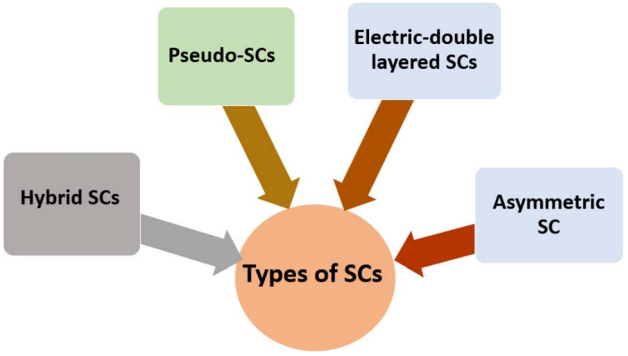

Fig. 11 Different types of SCs.

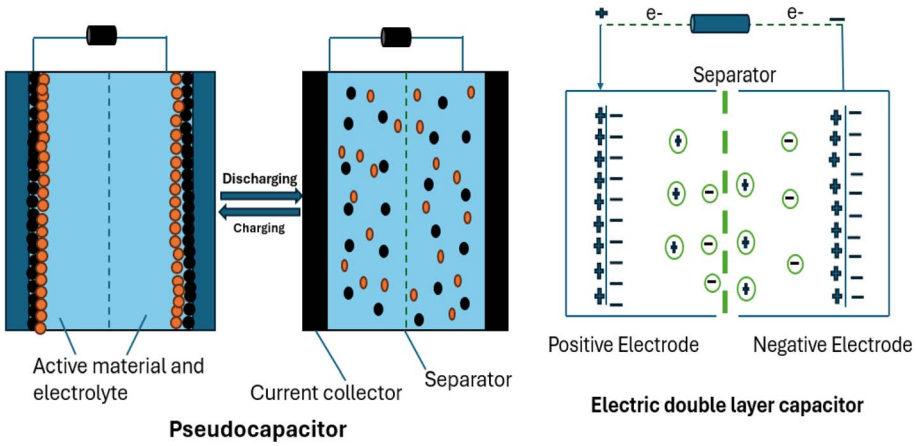

Fig. 12 Structure of pseudocapacitors and electric double-layer capacitors (redrawn and modified from open source).[147]

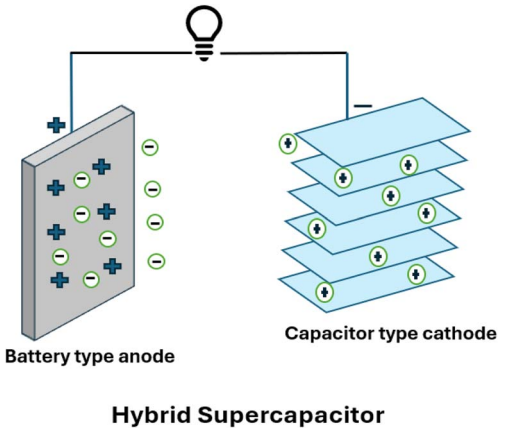

Fig. 13 Structure of hybrid SCs (redrawn and modified from open source[147]).

solid-state electrolytes are frequently used electrolytes. Aqueous electrolytes can increase ionic concentrations and decrease resistances, which increases capacitance and power density.[154] Because of their greater operating potential, organic electrolytes, that is, solutions based on ammonium cyanide, can be used in industrial SCs. Aqueous electrolytes have many benefits over organic electrolytes, as shown in Fig. 14, including lesser toxicity, greater safety, and cost-effectiveness, even if they have a lower voltage.[142]

Owing to their minimal energy density compared to the organic solution, the aqueous solution's limited working potential is one of its most significant drawbacks in application. Significant energy densities are hard to come for these aqueous electrolytes due to their narrow voltage window. The industry is waiting for a more effective energy storage technology to keep up with the rapid advancements in electric cars and other electronic devices. The scale issue and rapid charging are the two main issues facing the EV industry.[155,156]

4.2 Polyaniline and its composites in SCs

According to Table 6, PANI is the significant CP which has been widely considered as an electroactive factor for energy storing

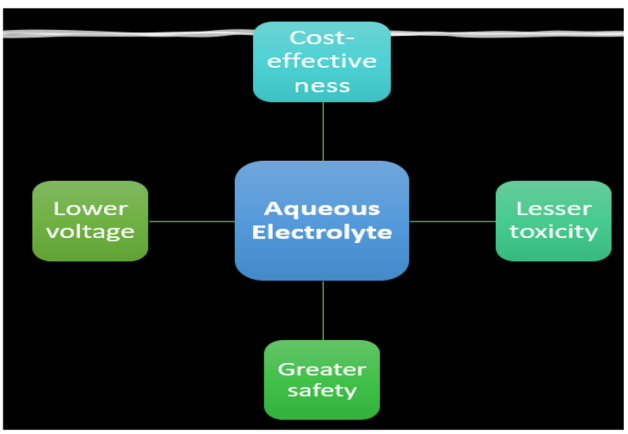

Fig. 14 Benefits of aqueous electrolytes over organic electrolytes.

capacitors, because of its extraordinary qualities, which include high electroactivity, ecological permanence, flexible electrical conductivity, high doping level, high processability, and promising electrochemical characteristics due to different oxidation states.[13] In the realm of flexible smart applications, one of the promising conjugated polymers that has received much study is PANI.[157,158] The use of PANI in smart applications such as gas sensors,[159] biosensors,[160] humidity sensors,[161] temperature sensors,[162] photoluminescence,[163] anti-corrosion,[160] transistors, pressure sensors,[164] LEDs, antenna, electrochromic displays, shape memory, absorbent/water purification, electrorheology, photocatalyst, electrical shielding, SCs, batteries, solar cells, nanogenerators, and fuel cells due to its extensive series of electrical conduction process.[165]

Quick charge–discharge kinetics, more economic, appropriate structure, and quick doping-dedoping routes are among PANI's benefits. Furthermore, n-dopable ($LiPF_6$) and p-dopable (HCl) PANIs have a higher power density and a superior resistance to deterioration.

PANI is a valuable material for additional research in the area of high-efficiency SCs because of its property.[179] The majority of published data for polyaniline-based SCs indicate that the charging and discharging process's operational window potential is among 0.8 and 1.0 V. Due to the low energy density achieved, PANI-based SCs with a hypothetical window below 0.6 V are not very appealing. A few research organizations began looking into PANI as an electroactive material for SC applications in the 1990s. Of these, Goswami *et al.* published the majority of the initial reports,[166] which were then followed by Arbizzani *et al.*, who picked up steam at the start of the twenty-first century.[180] The majority of reported scientific articles so far have used PANI as a composite form.[166] Moreover, PANI has been noted as an effective SC electrode in the absence of processing composites. Additionally, the only utilized material as electrode is PANI because of its several redox states, which can generate an extensive charge potential when switching between oxidation states during cycles of charging and discharging.[181]

For high-grade SCs, Gao *et al.* have recently described a systematically porous carbon microsphere (SCM)/PANI electrode. SCMs were created by flaming a chitin/chitosan mixture solution, where chitosan was utilized to make the nanopores and nanochannels that made up the microspheres.[182] Another intriguing material for making PANI composite SC electrodes is carbon black (CB). Bavio *et al.*[183] has stated a comparatively extreme specific capacitance of approximately 1500 F g^{-1} for SC electrodes with a composite PANI/CB nanostructure. PANI/CB nanostructures were created by simply adding carbon black (0.1 mg mL^{-1}) to the polymerization solution's original aqueous dispersion.

S. Goswami *et al.*[184] have recently reported on the use of CB integrated into the PANI matrix to fabricate a high-performance SC electrode using a PANI nanostructure. The CB that was utilized was made from the carbon waste from regular cooking ovens.[183] Prasanna *et al.* used a three-electrode setup and a 1 M H_2SO_4 electrolyte solution to investigate the redox activity of PANI and PANI/SnO_2 nanocomposites (Fig. 15). At 0.48 and 0.35 V, two redox peaks are visible for PANI and the same type of

Table 6 MO_x@CP-based composites for electrochemical application (SCs)[33,147,166–168]

CPs	Method	Energy application	Specific storage capacity (F g^{-1})	Power density (W h kg^{-1}, μW cm^{-2})	Capacitance retention	Ref.
PANI/RuO_2	Atomic layer deposition	Offer high energy storage capacity and enhanced redox efficiency	710	10/42.2	88% after 10 000 cycles	169
PANI/Fe_2O_3	Hydrothermal synthesis combined with *in situ* polymerization	High electrochemical performance and enhanced energy storage capabilities	1124 at 0.25 A g^{-1}	14.4 and 58	82% following 10 000 cycles	170
MnO_2/PANI	Electrodeposition method	Enhanced electrochemical performance in energy storage devices, particularly SCs	248.5 at 1 A g^{-1}	88.4 and 800	>97.7% after 5000 cycles	171
PPy/Fe_2O_3	Hydrothermal and electrochemical polymerization	High electrical conductivity, stability, and electrochemical performance, making them suitable for SCs and batteries	1167.8	42.4/9.14	97.1% after 2000 cycles	172
PPy/rGO	Chemical polymerization	Enhanced conductivity, flexibility, and high specific capacitance, making them valuable for SCs and battery electrodes	197.6	61.4	78% following 2000 cycles	173
PPy/CuO	Polymerization	Synergistic conductivity, high specific capacitance, and redox activity, making them suitable for SCs and LIBs	—	—	—	174
PPy/CoO	CoO developed using PPy on 3D nickel foam	High conductivity, electrochemical stability, and excellent pseudocapacitive behavior	2223	43.5/5500	99.8% after 2000 cycles	175
PPy/$ZnCo_2O_4$	Chemical polymerization	High conductivity, large surface area, and superior electrochemical performance	—	—	—	169
PPy/GO	Electrochemical co-d position	Offering improved conductivity, flexibility, and extreme specific surface area, compelling them ideal for SCs and flexible energy devices	152	12.9/954	96.4% following 5000 cycles	176
PPy/LiV_3O_8	Oxidative polymerization *in situ*	High energy density, stability, and enriched electrochemical efficiency, particularly for LIBs	—	—	—	175
PPy/TiO_2	Heat treatment, reduction, and direct mixing/drying	Perfect for advanced SCs and photocatalytic energy storage applications because of their excellent conducting power, large area of coverage, and stability	—	—	76.5% following 100 cycles	169
PTh/rGO	In situ polymerization	Enhanced electron mobility and stability in SCs applications	971 at 1 A g^{-1}	38.11 and 7000	98% after 10 000 cycles	177
PTh/$LiClO_4$	In situ polymerization	Ionic conductivity and enhanced electrochemical stability in LIBs	255	—	—	178
PTh/TiO_2	In situ polymerization	Stability and photocatalytic ability of TiO_2, making them ideal for energy storage, photocatalysis and photovoltaics applications	1533	—	—	109

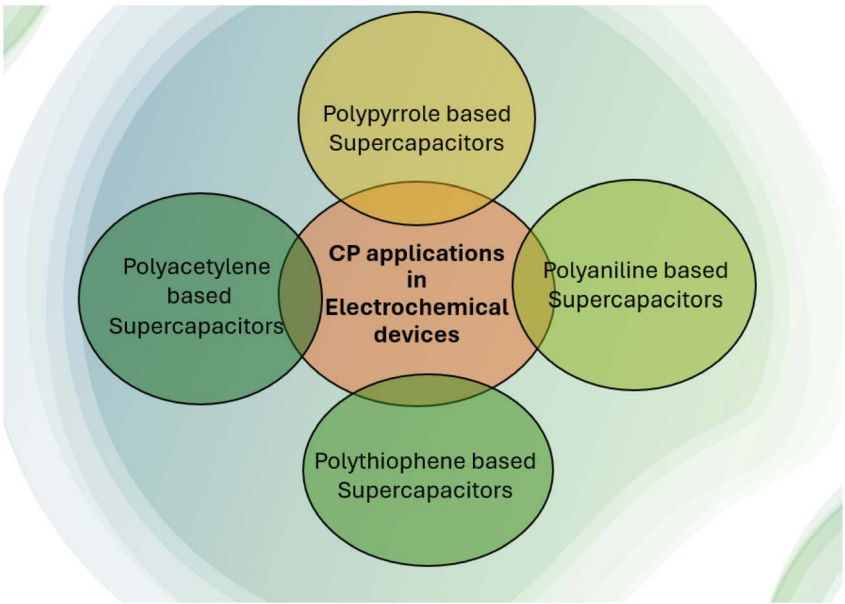

Fig. 15 CP (PPy, PANI, PTh, and PA) applications in electrochemical devices.

anodic curve with some peak altering is visible for PANI/SnO_2 nanocomposites at 0.22 and 0.6 V. The anodic curve changing, which results from SnO_2 oxidation and electrode resistance, indicates that SnO_2 is present in the nanocomposites.[185]

Recent work on carbon nanofibers by Tian and colleagues produced N-doped carbon nanotubes/PANI composites. Based on the categorized core-sheath structure of N-CNT/PANI/CNT fibers, they developed a wearable SC that, after 10 000 series, has a specific capacitance of about 320 F g^{-1} at 1 A g^{-1} over 92% of the retaining factor.[175] SCs are made flexible by a well-aligned CNT fiber, and their permeable N–carbon nanotube structure considerably facilitates the relocation of ions and electrons that improve their storage behavior. Clothing made from carbon fibers or nanofibers has a lot of potential as an electrode material for malleable SCs due to its elevated electrical conductivity, large surface area, and good chemical strength. However, a straightforward and inexpensive method can be used to readily build a PANI nanostructure on carbon fibers for use as a variable SC electrode.[186]

4.3 PANI and its application in batteries

PANI has been extensively studied for over 150 years in various applications due to its wide range of functions, and it was only around fifty years ago that PANI was 1st used in an electrochemical application. Chemical doping is a natural method for CPs such as PANI to change from insulators to semi-metallic conducting.[187] PANI and its derivatives are used in batteries because of their ability to conduct metals and function as lenient polymeric networks that provide high elasticity, exceptional mechanical power, and simple functionalization synthesis. Therefore, PANI is being looked into as a possible cathode material option for LIBs, as explained in Table 6.[188]

As compared to PANI with other CPs, such as PPy and Poly(3,4-ethylenedioxythiophene) has capacity of 114 and 115 mA h g^{-1}, reveals that PANI has a complex hypothetical capacity (294 mA h g^{-1}) as LIB cathode material. $LiPF_6$, $LiBF_4$, $Zn(ClO_4)_2$, $LiClO_4$ and other ionic salts have been used as dopant materials for PANI in order to create the cathode electrode for LIBs.[189]

Additionally, sophisticated hybrid cathode materials that combine PANI with organic and inorganic materials such as $LiMn_2O_4$, MOS_2, graphene (G), V_2O_5, $LiFePO_4$, polyoxometalate, or reduced graphene (rG) are being investigated as a way to recover the electrochemical characteristics of battery cells. Ajpi[188] and colleagues have found that when $LiFePO_4$ (120 mA h g^{-1}) or pristine PANI (95 mA h g^{-1}) cathode systems are compared, the hybrid $LiFePO_4$@PANI exhibits a substantially enhanced capability of 145 mA h g^{-1} at a redox rate of 0.1C. Hybridization causes the contact resistance to decrease, which speeds up the diffusion of lithium cations to the electrolyte and the transmission of electrons to the collector along the polymer chain.[116,163,190] In addition to the electrode component used in LIBs, PANI-based hybrid composites have been developed for lithium sulphur (Li–S), aluminum (AIB), sodium (SIB), zinc ion batteries (ZIBs), and ammonium storage cells, among other battery cell types.[159] Huang *et al.*, for example, reported on the production of PANI-inserted MnO_2 nanolayers with 40% utilization rate using them as the cathode material for Zn–MnO_2 rechargeable devices.[14] The nanolayers were stabilized for 5000 cycles using a slight aqueous electrolyte. Additionally, a number of studies have been published on PANI composites for magnesium-ion batteries.[159,191] Wang *et al.* have recently revealed that a flexible cathode for MIBs using PANI nanoarrays and carbon cloth has 97.25% retention capacity at 1 A g^{-1} after 1500 phases.[171] However, Krishna *et al.* have revealed that PANI has electrocatalytic action in Mg–S batteries. The MgS_x catalyst was loaded onto pristine carbon cloth (CC) to create one electrode, while the PANI-coated carbon cloth was

Table 7 Battery applications of polyaniline CPs[166,181]

CPs	Synthetic method	Energy application	Energy storage	Ref.
PANI/$LiFePO_4$	Polymerization *in situ*	LIBs 5C, St: 76.8% retention	Discharge capacity specific to 0.1C and ability to reverse occur at 163.0 and 125.3 mA h g^{-1}	187
PANI/Li	Polymerization *via* chemical oxidation	LIBs	Discharge rate 37 mA h g^{-1} and 99.99% strength over 50 cycles	189
MoS_2/PANI	Polymerization	LIBs anode	915 and 369 mA h g^{-1} at 1 and 4 A g^{-1} are the reversible capacities. 200 cycles later	159
PANI/rGO	Polymerization	LiSB	Following 200 cycles, there is 600 mA h g^{-1} of stable capacity and 1548 mA h g^{-1} of reversible capacity at 0.05C	193
3D G/PANI/ polyoxometalate	Polymerization *in situ*	LIBs rechargeable	135 mA h g^{-1} reversible capacity; zero specific capacity-decay rates	116
PANI/MnO_2	Polymerization *in situ*	ZIB	The discharge capacity (at 0.2 A g^{-1}) and dropped level were at 210 and 110 mA h g^{-1} after 200 cycles	109
PANI/V_2O_5	Polymerization *in situ*	Acts as SIB cathode	153 mA h g^{-1} of reversible capacity at 0.3C; 73.3% of capacity retention after 1000	14
$LiFePO_4$/PANI	Mixing physically	As a LIB cathode	Discharge capacitance (0.1C) is 145 mA h g^{-1}	188
PANI/Al_2O_3	Mixing physically	Aluminum-ion batteries	200 milliampere-hours per gram at one ampere-hour; stability 0.003% capacity degradation each cycle over 8000 cycles	191
PANI/V_2O_5	*In situ* hydrothermal reaction	Zinc-ion batteries	Early discharging rate is 275 mA h g^{-1} at 5 A g^{-1}, and the St is 208 mA h g^{-1} at 2000 cycles	191
PANI/V_2O_5	Polymerization *in situ*	Zinc-ion batteries	353.6 mA h g^{-1} reversible capacity at 0.1 A g^{-1}	149
PANI/MgS_x/TiO_2	Polymerization *in situ*	Mg–S batteries	After 30 cycles, the retention is 495 mA h g^{-1}, or around 97% of the early reversible rate of 510 mA h g^{-1}	192
PANI/V_2O_5	*In situ* polymerization	Mg ion batteries	Reversible capacity: 115 mA h g^{-1} at 0.1 A g^{-1}	163
PANI/Fe_2O_3	—	LIBs SIBs	Retained after 50 cycles at 982 mA h g^{-1}	109
PANI/LIV_3O_8	Chemical oxidative polymerization	LIBs	997 mA h g^{-1} 95% after 55 cycles	194
PANI/ $LI(Ni_{0.8}Co_{0.1}Mn_{0.1})O_2$	Procedure of solution	SIBs	After 80 cycles, 96.25%, or 193.8 mA h g^{-1}	195
TiO_2/GO/PANI	—	LIBS	435 mA h g^{-1} after 250 cycles 1335 mA h g^{-1}	190

used to create the other. The superior electrochemical performance of MO_x@PANI is attributed to improved electrical conductivity due to synergetic effects, enhanced lithium ion diffusion and good structural stability, which make it an excellent candidate for battery applications (Table 7).[192]

4.4 PPy and its composites in SCs

One of the CPs that is most typically utilized for a range of applications is PPy. The electrochromic effect based on electrochemical polymerization conditions, solid absorptive characteristics towards DNA, gases, and proteins, corrosion-free qualities, redox activity, catalytic movement, capacity to synthesize nanowires through conductivity ranging between 10^{-2} and 10^{-4} S cm^{-1} at 27 °C, ion discrimination skills and ion exchange, charge/discharge methods, and electrochromic effect define this polymer's versatility.

Most of these characteristics are based on the makeup of the dopant as well as the synthesis method. Electrochemical synthesis and deposition of PPy are possible on the conducting surfaces. The low cost, easy fabrication, high conductivity, customizable doping/dedoping features, and extensive range of uses of PPy have drawn several investigation considerations in fields such as electrical devices, sensors, and energy storage devices. Of the several CPs, PPy is the one that has been studied the most because of its favorable redox properties and ease of manufacture. Because of the powerful intrinsic qualities listed above, PPy has great potential for various applications including sensors, artificial muscles, batteries, SCs, and microwave shielding. This well-known PC can store more charge because of the inherent properties of the faradaic storage technology.[116]

PPy-based material composites are extensively researched for many uses. Owing to its important characteristics, such as high conductivity, high capacitance, and low density, PPy can be employed as a material that works well for SC applications. Chemical and electrochemical processes are the primary means of developing PPy. When a large amount needs to be generated, chemical synthesis is performed, and potent oxidizing agents are required. Electrochemical production is recommended for research purposes due to its ease of use, precision in controlling material thickness, geometry, and position, flexibility in doping

materials during synthesis, accessibility to a wide range of dopant ions, and production of high-value films. It creates adherent surface uniform deposits when monomer units are in a bulk solution.[196,197]

Younghee and colleagues analyzed the development of a unique 3D hybrid nanoarchitecture by physically inserting monodisperse PPy nanospheres as client species into piled graphene layers without significantly altering their appearance. At a weight ratio of 8/1 between PPy and graphite, the precursor of graphene, the graphene/particulate PPy (GPPy) nanohybrids showed excellent electrochemical functioning in relation to charge transfer resistance, chemical reaction activity and Cs. This was influenced by the proportions and makeup of the PPy tiny spheres. Bulkiness or density of packing dictated the execution result of the electrode materials. Using an acidic electrolyte, flexible and solid-state hybrid capacitor cells showed outstanding electrochemical accomplishment, with a maximum energy density of 8.4 W h kg^{-1} or 1.9 W h L^{-1} and a maximum power density of 3.2 kW kg^{-1} or 0.7 kW L^{-1}. The cesium in the 6 mol L^{-1} KOH solution is approximately 433 F g^{-1} at the optimal PPy intensity in the PPy/C aerogel nanocomposite (35 weight percent of PPy). This is due to the substance of the nanocomposite's double-layer and redox capacitive behaviour working together. Activated carbon (AC) and PPy composite electrodes show relatively high cesium, or 45.1 F g^{-1}, in a separate report by Thakur *et al.* This is approximately twofold as high as other standard SCs based on activated C electrodes.[198]

PPy/NiCoHCF (nickel-cobalt hexacyanoferrate) was synthesized by Wu *et al.* using an electrochemical process with an inexpensive corrosion-resistant steel template. The findings demonstrate that by adding NiCoHCF to PPy, its charge storage qualities were enhanced in both non-aqueous and aqueous environments. The proposed nanocomposite, based on the galvanostatic charge–discharge method, could achieve extreme charge storage capacities of 529 and 668 F g^{-1} in both aqueous and non-aqueous ionic solutions. Additionally, at a current density of 10 A g^{-1}, the nanocomposite showed a remarkable specific energy density of 87 W h kg^{-1}, a remarkable specific power density of 5600 W kg^{-1}, and excellent strength with <10% loss after 1000 cycles. The conclusion indicates that the suggested nanocomposite could be a valuable electrode material for electrochemical SCs.[199]

SCs ability to supply at high momentary durations has led to their use as electrical energy storage devices. Nanocomposites composed of MoS_2, graphene, PPy, and other filler elements are the advanced items for SC purposes. The exceptional electrical conductivity and higher surface volume of these materials, which are essentially 2D, allow them to function exceptionally effectively in SCs.[200] SC applications of numerous MO_x@PPy-based composites are discussed in Table 6.

5 Electrocatalytic applications

The sensible creation of long-lasting, highly effective catalysts that are also reasonably priced and readily available is essential to electrocatalytic water splitting. Therefore, it is necessary to have an effective electrocatalyst that can successfully follow the electrolytic catalysis of the HER and OER.[18] Fuel cells, which operate on hydrogen or H-rich fuels and release little CO_2, have become potential energy conversion technologies.[87] The superior qualities of membrane fuel cells (PEMFCs) and proton trade, including their extreme energy conversion efficacy, elevated open-circuit potential, partial fuel edge properties, and effective low-temperature electrochemical oxidation of natural molecules such as ethanol, methanol, and formic acid have drawn more attention to them than to the others.[201] Furthermore, the fuel cell's stability and efficiency have been linked to the enhanced 3-phase interface, which consists of an ionomer—an ionic solution membrane—attached to the surface of the catalyst. At the solid–electrolyte interface, protons are available to the electrolytic stage and react with O_2 after initially reacting with the anode's solid phase and hydrogen gas molecules.[202] Therefore, creating stable, affordable electrocatalysts and polymer membranes, as well as comprehending the efficiency of small organic molecules' catalytic activity, is essential for fabricating fuel cells that are both large scale and economic.[19]

For fuel cell applications, CPs such PPy, PANI, poly-3-methyl thiophene (PMT), and PEDOT have been effectively employed as electrocatalyst-supporting materials. The unusual, conjugated architectures of CPs, which have remarkable chemical strength, extreme electrical conduction, ease of production, and cheapness, have shown promise in their use as catalytic supports.[203] The electrolytic oxidation of tiny molecules including H, CH_3OH, and HCOOH has thus been accomplished (Fig. 16), employing CP-based nanohybrids, which are composed of a succession of metal or MO_x added on the surface of the polymer. Recent efforts to develop electrode materials have involved the direct deposition of nanostructured metal catalysts on CP substrates or on customized polymer nanostructures.[204] Hydrogen's exceptional qualities make it a desirable clean energy source.[205] Hydrogen has zero emissions when used as a fuel because it generates energy with just water vapor as a byproduct.[206] This special quality makes hydrogen a strong candidate in the drive to decarbonize in various fields[207] including power generation,[191] transportation,[208] and industries.

Apart from its advantages for the environment, hydrogen has a high energy density that can compete with traditional fossil fuels.[209] Because of this feature, it is a desirable choice for applications where transportation efficiency and energy storage are crucial. A move towards alternate feedstocks, such as wastewater and saline water, which not only provide a sustainable resource but also pose unique problems that call for creative solutions, has been spurred by the necessity to match hydrogen production with sustainability objectives.[210] Researchers are looking into unusual water sources, especially wastewater and salt water, as possible feedstocks in the pursuit of sustainable hydrogen synthesis.[211] Although these sources provide a plentiful and sustainable supply, using them presents a number of complex issues that need creative solutions for effective and ecologically conscious hydrogen production. Complex Chemistry of Water: The chemical compositions of wastewater and saline water are frequently complicated and

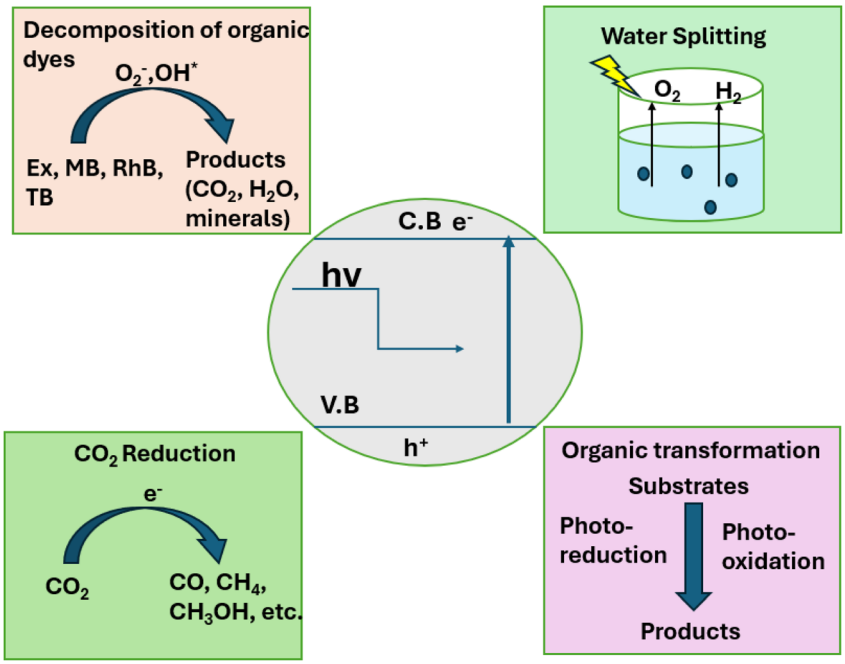

Fig. 16 Overview of the Pi-conjugated polymer for multiple photocatalytic activities.

varied, containing dissolved ions, pollutants, and impurities.[212] Designing catalysts and procedures that may effectively and selectively extract hydrogen while minimizing undesirable side effects is difficult due to this intricacy. Corrosion and fouling: equipment and catalysts may corrode and foul due to the corrosive properties of salty water and the presence of contaminants in wastewater.[177]

5.1 Hydrogen evolution reaction

The most significant method for archiving the next creation of green power is the HER, which is the cathodic reaction in the H_2O-splitting route.[105] In addition to Pt, which is the utmost potent HER catalyst in acidic media, a number of low-cost metal phosphides, nitrides, transition metals (TM), and TM dichalcogenides have been investigated as possible HER catalysts in alkaline media.[213] Due to their reduced asset costs when contrasted to acidic electrolytes that depend on Pt or alkaline electrolyzer, additional noble metal-based electrocatalyst development is being actively studied.[214] CPs are becoming competitive alternatives to the HER as both photocatalysts and electrocatalysts, despite the fact that a majority of studies on novel electrocatalysis resources have concentrated on TM-based reagents. For example, in order to create keto-indoleamine hydrogen bonds, polydopamine (PDA) was successfully altered with indoleamines, giving the HER a favorable H adsorption energy.[215]

According to the DFT simulations, this bond, which is created when o-dopamine quinone and aminochrome parts are linked, shows hydrogen bonding near zero and is said to be advantageous for driving the HER.[216] Moreover, the HER activity can be further adjusted to attain CP performance equivalent to Ni by varying the degree of functionalization. Similarly, two pyridinic N were added to the structure of dibenzo thiophene sulfone, which improved the resulting polymer's photocatalytic activity. In a different investigation, PPy doped with I2 demonstrated competent activity as a supporting electrode for the HER.[171] Additionally, I2 doping produced electrodes with higher conductivity and stability. MoS_2/PANI was produced by Ding and colleagues by combining MoS_2 nanosheets with the PANI matrix, which was earlier made using a hydrothermal technique. With an optimal composition that contained 19 wt% of PANI, the MoS_2/PANI composite demonstrated a higher activity than that of MoS_2. Even though MoS_2 aggregation reduced the number of effective sites, the greater electric conduction resulted in better performance. Likewise, Torres and associates created Ni/PANI hybrid electrodes by electrodepositing Ni in dissolved PANI.[217] These conductors showed a thirty percent increase in electrical conductivity at 100 mV *vs.* RHE in an alkaline electrolyte associated with the bare Ni substrate because of enhanced nickel dispersal in the PANI matrix, which promotes H-movement to the Ni sites. A similar process was utilized to produce Pd/PANI or Pd/PEDOT nanocomposites.[218]

Furthermore, CPs have been used with additional materials to produce hybrids that work together as TM-based catalysts. For instance, PANI was coated on $Na_4Ge_9O_2$ to support Pt nanoparticles, and Ir has been reinforced with TiO_2/TiO_2-WO_3 essential elements to create hybrid sustenance for NiP. For the latter, a reported 80 mV drop in overpotential was ascribed to PANI's electrical conductivity in the alkaline electrolyte in a deprotonated form. Furthermore, PPy was used to encapsulate carbon nanotubes (CNTs), which helped immobilize and disperse Co_3O_4 nanoparticles.[219] The polymerization of CPs using electrochemical or organic pathways with the inclusion of

Table 8 Summary of MO_x@CP catalysts used in the HER, ORR, and OER, highlighting their performance in different electrolytes[222]

Reactions	Catalyst	Electrolyte	Feature	Ref.
HER	PANI/MoS_2 – PPy/MoS	0.5 sulphuric acid	Overpotential at 10–280 mA cm^{-2}	219
	Co_3O_4/PPY/C	1–4 M potassium hydroxide	—	223
	PSS-PPy/Ni–Co–P	0.10 M KOH	490 mV	224
	$FeCo_2O_4$/$FeCo_2S_4$/PPy	1 M KOH	67 mV	186
	Pt/$Na_4Ge_9O_20$/PANI	0.5 M H_2SO_4	98.3 mV	149
	PPy/$ZnWO_4$	0.5 M H_2SO_4	543 mV	225
ORR	$MnCo_2O_4$/PPy hybrid	0.1 M KOH	800 mV	226
	Co_3O_4/PANI		700 mV	227
OER	PPy- ionic liquid	1 M KOH	328 mV	228
	$CoFe_2O_4$/PPy	0.1 M KOH	274 mV	229
	Co_3O_4/PPy/MWCNT	0.1 M KOH	340 mV	224
	$Co(OH)_2$/PPy/GO	0.1 M KOH	120 mV	230
	$Ni(OH)_2$/PPy	0.1 M KOH	350 mV	231
	Ni/$NiFe_2O_4$@PPy	0.1 M KOH	272 mV	91
	$FeCoNiBO_x$/PPy/rGO	0.1 M KOH	370 mV	232
	Sm_2O_3@PPy	0.1 M KOH	461 mV	18

NPs or additional components is another widely used method. For instance, aniline was electro-polymerized on Ni foam-supported zeolite to create a PANI/zeolite/nickel froth cathode.[220] The HER activity was increased when zeolite/Ni was coated with enough PANI layers, highlighting the significance of managing the polyaniline amount and coatings generated to attain peak execution exclusive of blocking availability to the zeolite's functional sites. Similarly, deposited monomers on NiCoP films were polymerized to cover PSS:PPy on NiCoP. By altering the metal atoms' electrical structure and surface shape, this technique made it possible to tune the activity of HER of NiCoP. Likewise, $FeCo_2O_4$@PPy, $FeCo_2S_4$@PPy, $ZnWO_4$@PPy and $Na_4Ge_9O_2$@PANI were found to have enhanced activity as a result of hybridization.[221]

Wang *et al.* showed that using organometallic materials to create polymeric complexes functional for the HER is a noteworthy tactic (Table 8). They created porphyrin Co parts, and Co that was linked to an imine ring performed better in the HER. Pyrolysis can be used to create a specific metal-like catalytic agent on the structures of carbon from metals that are widely distributed in a polymeric matrix.[221] Metallopolymers having a metal at the center linked to ligands holding heteroatoms that are nitrogen or sulphur are created using the commonly used post-calcination synthesis technique. In comparison to cutting-edge metal-based catalysts, calcined catalysts are typically more competitive and have greater HER activity than the non-calcined ones. CPs function as precursors in this case, losing their structure when calcined.[109]

Mendoza *et al.* claimed that techniques that incorporate metal traces on the CP scheme, polymer covering of metal NPs, or immediate polymer and NP manufacturing are generally more efficient than simple routine mixing. To achieve structures that support charge passage, especially ion flow across the complete conductor, material production must be optimized. Thick polymer films may make it harder to reach the metal sites, even though coating polymers on transition metal NPs can improve the intrinsic activity and electrode conductivity of metal nanoparticles. Thus, one of the biggest obstacles to producing more active composite materials is still developing interfaces in nanocomposites.[222]

5.2 Oxygen reduction reaction

Power transformation equipment such as fuel cells and batteries made of metallic-air depends on the ORR, a process that is critical to biological systems and necessary for maintaining life.[177] Because the ORR at the cathode has a slow kinetic, it has a substantial impact on the device efficiency of proton exchange membrane fuel cells, particularly direct methanol booths.[233] Triplet molecular oxygen's (O_2) distinct electrical structure is the cause of this slow reaction. Anti-bonding impoverished molecular orbitals are occupied by unpaired electrons, which prevent new electrons from entering. In order to promote electron transference and lower extreme potential involved in the ORR, catalysts that dynamically adsorb molecular oxygen must be improved.[234]

The ORR can move forward *via* either an outer-sphere or an inner-sphere process. Through a two-electron transfer, the outer-sphere mechanism produces H_2O_2 as the only product. Simultaneously, synergistic or disruptive assimilation of the molecular O_2 atom is a part of the inner-sphere mechanism. Although the last splits the O–O bond to produce H_2O with four-electron transmission, the first maintains the oxygen–oxygen bond and produces H_2O_2 (two-electron transfer). The favored channel for CPs is a two-electron transfer. CPs frequently behave as electron donors, transferring charge to bound oxygen molecules in a powerful way. By changing the molecular symmetry and lengthening the O–O bond, this interaction activates oxygen. Furthermore, CPs can oxidize to a significant degree, converting absorbed O_2 to O_2 (ref. 134) The increased catalytic activity of nanocomposites made with metal NPs and CPs is frequently ascribed to the interaction of the metal activity with the increased electrical permeability of the matrix of polymeric material within the electronic potential border.[163]

Zhou and companions used polypyrrole and the TM oxide $MnCo_2O_4$ to create an ORR catalyst. Interfacial polymerization

with oxidative chemicals was used to fabricate the material. Using RRDE analysis, they confirmed that when PEDOT was used alone, the reaction process changed from a 2-electron transport to a 4-electron movement once the material was included into the matrix of the polymer. Using cyclic voltammetry to evaluate the substance's firmness, they discovered that the hybrid-modified transparent carbon electrode retained signal integrity even after 500 cycles of applied potentials between −1.0 and +1.0 V.[235] The overpotential was lower in electrochemical experiments than in each $MnCo_2O_4$ and PPy materials. Additionally, instead of the limited 2-electron transference seen when utilizing only the polymer, they found a 4-electron transfer channel employing a rotating ring-disk electrode (RRDE).[227] The electrocatalytic performance showed impressively little alteration (1%) even after 16 h of continuous process. By mixing PEDOT with $CoMn_2O_4$ in a wet manner, Chowdhury *et al.* created a hybrid catalyst for the ORR. There was an overpotential of −870 mV in the resulting composite material.[236]

5.3 O_2 evolution reaction

The OER is a vital electrolytic route that is essential to the parting of H_2O to produce H. Because of extremely corrosive circumstances, this several-phase method which involves the movement of 4 protons connected to 4 electrons stays slow and complicated, exhibiting large overpotentials and restrained strength.[237] The continuous search for long-lasting and efficient OER electrocatalysts has drawn a lot of attention towards TM-based catalysts, particularly spinel oxides, TM hydroxides, and perovskite oxides, which are prized for their remarkable activity and affordability.[238] Improving these materials' conductivity and stability is still crucial, though. An interesting approach in this regard is to incorporate conductive materials such as CPs into these electrocatalysts to improve stability and promote charge transfer. Numerous composite materials made of polymers and MO_x have been described recently. To fully utilize CPs' potential as OER electrocatalyst components, more research is necessary.[229] $MnCo_2O_4$/PPy, $CoFe_2O_4$/PPy, Co_3O_4/PANI, Co–Fe/PANI, Co_3O_4/PEDOT, Co/PTh, NiO/poly(3-hexylthiophene), $Co_2(OH)_3$/Poly(3-bromo-thiophene), MnCo-oxides/PEDOT, and Co_3O_4-polyethyne have all been produced through various techniques.[192] Enhanced catalytic efficiency of the hybrid electrolytic catalysts has been observed in these research studies.

This improvement is ascribed to the many electrical routes provided by the CPs, the modifying-tuning of the activity of metal catalytic routes, and the more extensive contact and dispersal of functional sites made possible by a matrix made of polymers.[91] Using $MnCo_2O_4$-NPs with PPy, for example, Cao *et al.* chemically polymerized pyrrole with H_2O_2 while the NPs were present to generate a composite. They found that the hybrid substance surpassed pristine materials in the OER, with an extreme potential of about 480 mV, which is similar to the benchmark for RuO_2/C (20%).[239]

The inclusion of PPy was attributed to the enhanced stability since it stopped $MnCo_2O_4$-NP corrosion and NP aggregation. Prior research on Co_3O_4 nanoparticles and PPy hybrids has clarified that the electrocatalyst's structure has a major impact on the composite's performance.[240] The most functional catalyst, they discovered, showed a great accessibility of Co-involved regions scattered throughout the matrix of polymers with an ideal CP quantity. A departure from this ratio caused the CPs to impede Co sites and cause nanoparticle aggregation.[160] A synergistic interaction is achieved by optimizing the molecular proportions of the composite components, which is echoed in other research studies producing Co_3O_4/PEDOT, Co_3O_4/Polyethylene, and Co_3O_4/PANI.[241]

5.4 Photocatalytic activity of PANI/ZnO hybrids

ZnO is a semiconductor of the n-type oxide that is eco-stable and nontoxic, with a high photo-activity and a strong bandgap energy.[242] It has the potential to acquire a unique and noteworthy capacity for photocatalysis over time, fascinating an important share of the solar band and exhibiting suitable photooxidation efficiency, including organic contaminants that are hazardous and non-biodegradable. ZnO, along with different semiconducting metal oxides, has several benefits and is a material that is good for the environment.[242] It is used in everyday applications without endangering the health of people or other living things. ZnO has good electrical features, strong mechanical capabilities, and great optical qualities. It is also less expensive than TiO_2NPs, which makes it a popular choice for large-scale operations. Fortunately, since light absorption is essentially limited to the UV range, ZnONPs' primary drawback is linked to their restricted spectral response.[243] As a result, significant efforts have been made to address both this drawback and the great characteristic potential of photogenerated charge carrier recombination. It is well known that the shape and morphological characteristics of semiconductor oxides have a significant impact on their ultimate photocatalytic efficiency.[244]

Representing the fabrication of novel and potent photocatalysts, which are distinguished by an efficient partition of the charge transferors, tremendous work and understanding of the requirements needed for synthesis are consequently essential. Superior consistency and reusability performance were achieved along with improved light absorption and volume-to-surface ratios. The primary characteristics are the final project's universality, the management of agglomeration and accumulation, and the removal of an infinite number of particles of catalyst following the photocatalytic phase in many stages.[245]

As previously stated, PANI, which is regarded as the most possible polymer systems for enhancing both the electrocatalytic and photocatalytic characteristics of ZnONPs, has drawn a lot of attention in a number of published studies aimed at boosting the photocatalytic effectiveness of ZnONPs through Vis-light. The fact that practically all of the works describe cationic methylene blue dye as an ecologically hazardous substance for examining the photocatalytic effects of blue light and UV radiation at room temperature is another intriguing finding.[246] Using an extreme amount of MB at a constant reaction rate, Qin *et al.*[245] found a higher photocatalytic activity of

a nanocomposite based on PANI-ZnONPs. An *in situ* chemical polymerization method was used to synthesize the PANI-ZnO hybrids, which serves as a necessary step in producing an effective photocatalyst. Additionally, the glassy carbon electrode was decorated with the resulting PANI-ZnO nanocomposite, and the potential of the PANI-ZnONPs/GCE terminal assembly as a microbial anode for fuel cells was also evaluated. PANI/ZnO nanocomposites were prepared by Asgari *et al.* in another published study.[247]

The observed outcomes of the photocatalytic reaction under visible light illumination suggest that the PANI/ZnONP catalyst surface has significantly degraded the MB dye. When it came to the destruction of the MB dye, the PANI/ZnO hybrid system demonstrated three times the photocatalytic activity of pure PANI. Similar to this, Rajeswari *et al.* created a nanocomposite consisting of PANI/ZnO and investigated its potential as a photocatalyst for the degradation of two dyes, MB and malachite green, in the occurrence of UV-Vis sunshine. The results demonstrated that a modest quantity of PANI/ZnO nanocomposite photocatalyst destroys all dye solutions (MB or MG) with 99% effectiveness after 5 hours of exposure to natural sunlight.[248]

The PANI/ZnO nanocomposite's photocatalytic capabilities for the artificial, broad-band antiseptic, non-decomposable, and highly H_2O-soluble breakdown of metronidazole (MNZ) were explained when exposed to UV and visible light. Consequently, there has been a lot of interest in treating wastewater before releasing MNZ into the environment. This work's challenge was to use a synthetic PANI/ZnO nanocomposite to eliminate MNZ from wastewater.[249] According to the data, the PANI/ZnO-based nanocomposite degraded MNZ at a pace more than 60 times faster than the plain ZnONPs photocatalyst. The significance of hydroxyl and superoxide anion radicals in the quick breakdown of MNZ is highlighted in Fig. 17.[250]

6 Future perspectives

While previous studies have provided significant insights into MO_x@CP composites, they have primarily limited on specific applications. The novelty of this review lies in its interdisciplinary approach, covering diverse areas such as biomedicine, energy storage, and electrocatalysis. Moreover, this work reinforces the synergy between synthetic strategies and functional performance, offering a roadmap for the systematic design of innovative MO_x@CP materials.

The features of innovative materials can be adapted to suit particular applications through the appropriate use of copolymerization, cross-linking, and ligand attachment. Further endeavors to foster interdisciplinary collaboration and create cutting-edge polymerization methods that reduce heterogeneity, enhance toxicity, and reduce manufacturing costs are desirable in the future. Despite the notable progress in MO_x@CP hybrid materials, various critical challenges must be addressed for their extensive adoption. Major obstacles involve complex protocols, high cost, and limited reproducibility at an industrial level. Developing an AI-driven material design, *i.e.* AI-designed CPs[251] and automated high-throughput screening, could facilitate the discovery of refined composites with enhanced performance. In addition, green synthesis routes such as solvent-free polymerization and bio-inspired fabrication are vital to uphold sustainable production while reducing environmental impacts.[252]

In biomedical applications, the toxicity of CPs and MO_x remains a key challenge, markedly for *in vivo* applications. Even if not all MO_x and CPs are resolved to be biologically safe, toxicity studies are currently being conducted.[253] Problems with sensor disposal, affordability, simplicity of manufacture, large-scale synthesis, and recycling must be tackled and resolved. In the light of electrochemical biosensors that provide a simple means of determining the concentrations of dangerous and

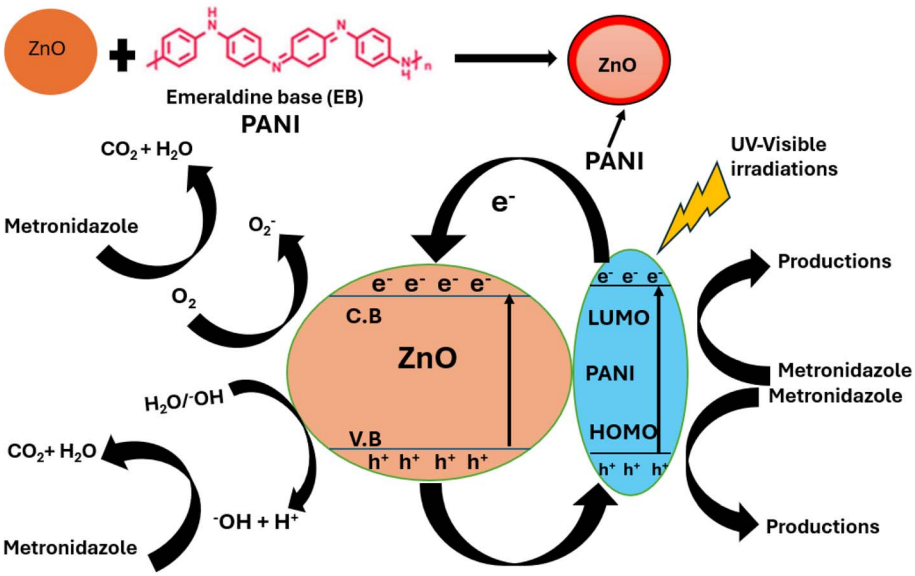

Fig. 17 Schematic representation of PANI/ZnO under UV-Vis light (redrawn and modified from source).[250]

harmful substances in the ecosystem, for public welfare and food security, monetization of these technologies is a crucial factor that needs to be considered. Sensors based on PANI integrate the feature of nanostructures and CPs. The primary issues preventing PANI from being widely used include non-degradability, insufficient solubility and improper processability.[157] As the need for quick, precise, and minimally invasive POCT devices for managing diabetes grow, new biosensing molecules are being discovered, improved, and created based on the subsequent advancements in technology. Because the majority of POCT devices for insulin and pancreatic hormone glucagon rely on retail available antibodies, there will be fewer sensing methods and devices available. As a result, there will be less flexibility in the selection of biosensing molecules, which will restrict the development of novel technologies in this area in the future.[254]

Although they face a number of significant obstacles, MO_x@CPs hybrids have a lot of potentials for electrochemical systems such as batteries and SCs. A significant challenge is maintaining stability over time under multiple charge–discharge cycles since physical and electrochemical stresses frequently cause component separation or structural damage. Another challenge involves reconciling the compromise between substantial power density (from CPs) and high density of energy (from MO_x), since maximizing one characteristic frequently puts the other at risk. Moreover, the inherent constraints of certain hybrids that usually have low conductivity might reduce the effectiveness of charge transfer. The synthesis of high-performance hybrids still faces challenges with scalability and cost-effectiveness, particularly when utilizing scarce precursors or intricate fabrication techniques. The creation of recyclable designs and green synthesis pathways is also necessary to ensure sustainable practices in their manufacturing and disposal, hence reducing their ecological mark. In order to overcome these obstacles, a multidisciplinary strategy combining materials research, engineering, and electrochemistry will be needed.[13]

MO_x-CP hybrids have promise, but there are a number of issues that must be resolved before they can be widely used in electrocatalysis. One major concern is how stable these hybrids will be over time in challenging operating environments including high voltages, high temperatures, and extreme pH, which can degrade materials and reduce catalytic activity. It is still technically challenging to achieve evenly dispersed and strong interface bonds among MO_x and matrix polymers because inadequate integration might impede electron transport and lower overall performance. Scalability is a further issue because large-scale production is restricted by the complexity, expense, and time required for the present synthesis processes. Furthermore, despite the fact that catalytic activity optimization has advanced significantly, commercial feasibility is still hampered by the conflict between efficiency and material cost. To overcome these obstacles, new material designs, scalable and environmentally friendly synthesis methods, and a deeper knowledge of mechanisms through experimental and computational methods will all be necessary.[232]

7 Conclusion

In summary, MO_x@CPs represent a promising class of multifunctional materials with revolutionary potential in biomedicine, energy storage, and environmental technologies such as photocatalytic water splitting. Their synergistic integration enables significant improvements in electrical conductivity, chemical and thermal stability, biocompatibility, and catalytic activity, making them ideal candidates for applications such as disease diagnosis, supercapacitor fabrication, and efficacious hydrogen production. This review emphasizes not only the recent advances in synthetic techniques—including *in situ* polymerization, sol–gel processing, and electrochemical deposition—but also the tunability of these materials for specific applications. Despite the impressive progress that has been made, several challenges persist, particularly in achieving uniform dispersion, enhancing interfacial compatibility, and scalable fabrication techniques. Sustained innovations in synthesis methods and material optimization will further unlock their full potential, progressive augmentation in these critical fields. Future research endeavors should prioritize designing smart and stimuli-responsive hybrids tailored for real-time biomedical applications. Additionally, machine learning and AI are integrated to predict the structure–property relationships for efficient rational design. With ongoing advancements in material design and fabrication techniques, MO_x-enhanced CP hybrids are equipped to make remarkable contributions to the development of viable technologies across various industries.

Data availability

No primary research results, software or code has been included and no new data were generated or analysed as part of this review.

Conflicts of interest

There are no conflicts to declare.

References

1 K. Namsheer and C. S. Rout, Conducting polymers: a comprehensive review on recent advances in synthesis, properties and applications, *RSC Adv.*, 2021, **11**(10), 5659–5697.
2 T.-H. Le, Y. Kim and H. Yoon, Electrical and electrochemical properties of conducting polymers, *Polymers*, 2017, **9**(4), 150.
3 X. Guo and A. Facchetti, The journey of conducting polymers from discovery to application, *Nat. Mater.*, 2020, **19**(9), 922–928.
4 T. Nezakati, A. Seifalian, A. Tan and A. M. Seifalian, Conductive polymers: opportunities and challenges in biomedical applications, *Chem. Rev.*, 2018, **118**(14), 6766–6843.

5 L. Yang, L. Yang, S. Wu, F. Wei, Y. Hu, X. Xu, *et al.*, Three-dimensional conductive organic sulfonic acid co-doped bacterial cellulose/polyaniline nanocomposite films for detection of ammonia at room temperature, *Sens. Actuators, B*, 2020, **323**, 128689.
6 N. V. A. Abhishek, A. Singh and T. Kumar, Metal-conducting polymer hybrid composites: A promising platform for electrochemical sensing, *Inorg. Chem. Commun.*, 2023, **154**, 111334.
7 D. N. Nguyen and H. Yoon, Recent advances in nanostructured conducting polymers: from synthesis to practical applications, *Polymers*, 2016, **8**(4), 118.
8 W. Tian, X. Liu and W. Yu, Research progress of gas sensor based on graphene and its derivatives: A review, *Appl. Sci.*, 2018, **8**(7), 1118.
9 Z. Farka, T. Jurik, D. Kovar, L. Trnkova and P. Skládal, Nanoparticle-based immunochemical biosensors and assays: recent advances and challenges, *Chem. Rev.*, 2017, **117**(15), 9973–10042.
10 S. Jafari, M. Dehghani, N. Nasirizadeh and M. Azimzadeh, An azithromycin electrochemical sensor based on an aniline MIP film electropolymerized on a gold nano urchins/graphene oxide modified glassy carbon electrode, *J. Electroanal. Chem.*, 2018, **829**, 27–34.
11 N. Shoaie, M. Daneshpour, M. Azimzadeh, S. Mahshid, S. M. Khoshfetrat, F. Jahanpeyma, *et al.*, Electrochemical sensors and biosensors based on the use of polyaniline and its nanocomposites: A review on recent advances, *Microchim. Acta*, 2019, **186**, 1–29.
12 Z. S. Saddique, F. Maleeha, B. Muhammad, Z. Sadia, A. Mujahid and A. Afzal, Core–shell niobium(V) oxide@molecularly imprinted polythiophene nanoreceptors for transformative, real-time creatinine analysis, *Nanoscale Adv.*, 2024, **6**(15), 3644–3654.
13 V. V. Vinayak, K. Deshmukh, V. Murthy and S. K. Pasha, Conducting polymer based nanocomposites for supercapacitor applications: A review of recent advances, challenges and future prospects, *J. Energy Storage*, 2024, **100**, 113551.
14 S. Zhang, X. Shi, X. Chen, D. Zhang, X. Liu, Z. Zhang, *et al.*, Large-scale and low-cost motivation of nitrogen-doped commercial activated carbon for high-energy-density supercapacitor, *ACS Appl. Energy Mater.*, 2019, **2**(6), 4234–4243.
15 K. P. Gautam, D. Acharya, I. Bhatta, V. Subedi, M. Das, S. Neupane, *et al.*, Nickel oxide-incorporated polyaniline nanocomposites as an efficient electrode material for supercapacitor application, *Inorganics*, 2022, **10**(6), 86.
16 J. Yesuraj, O. Padmaraj and S. A. Suthanthiraraj, Synthesis, characterization, and improvement of supercapacitor properties of NiMoO4 nanocrystals with polyaniline, *J. Inorg. Organomet. Polym. Mater.*, 2020, **30**(2), 310–321.
17 V. Babel and B. L. Hiran, A review on polyaniline composites: Synthesis, characterization, and applications, *Polym. Compos.*, 2021, **42**(7), 3142–3157.
18 A. M. Tawfeek, K. Jabbour, A. G. Abid, M. U. Nisa, S. Manzoor, B. Shabbir, *et al.*, Sm2O3 supported on conducting polymer (polypyrrole) as a highly potent electrocatalyst for water splitting, *J. Sol-Gel Sci. Technol.*, 2024, 1–14.
19 C. Santoro, C. Arbizzani, B. Erable and I. Ieropoulos, Microbial fuel cells: From fundamentals to applications. A review, *J. Power Sources*, 2017, **356**, 225–244.
20 M. Alsultan, A. M. Ameen, A. Al-Keisy and G. F. Swiegers, Conducting-polymer nanocomposites as synergistic supports that accelerate electro-catalysis: PEDOT/Nano Co3O4/rGO as a photo catalyst of oxygen production from water, *J. Compos. Sci.*, 2021, **5**(9), 245.
21 B. Guo and P. X. Ma, Conducting polymers for tissue engineering, *Biomacromolecules*, 2018, **19**(6), 1764–1782.
22 M. Tomczykowa and M. E. Plonska-Brzezinska, Conducting polymers, hydrogels and their composites: Preparation, properties and bioapplications, *Polymers*, 2019, **11**(2), 350.
23 J. G. Ibanez, M. E. Rincón, S. Gutierrez-Granados, M. Chahma, O. A. Jaramillo-Quintero and B. A. Frontana-Uribe, Conducting polymers in the fields of energy, environmental remediation, and chemical–chiral sensors, *Chem. Rev.*, 2018, **118**(9), 4731–4816.
24 N. Maity and A. Dawn, Conducting polymer grafting: Recent and key developments, *Polymers*, 2020, **12**(3), 709.
25 L. B. Kenry, Recent advances in biodegradable conducting polymers and their biomedical applications, *Biomacromolecules*, 2018, **19**(6), 1783–1803.
26 A. Eftekhari, L. Li and Y. Yang, Polyaniline supercapacitors, *J. Power Sources*, 2017, **347**, 86–107.
27 M. Beygisangchin, S. Abdul Rashid, S. Shafie, A. R. Sadrolhosseini and H. N. Lim, Preparations, properties, and applications of polyaniline and polyaniline thin films—A review, *Polymers*, 2021, **13**(12), 2003.
28 Y. Xie, Fabrication and electrochemical properties of flow-through polypyrrole and polypyrrole/polypyrrole nanoarrays, *Chem. Pap.*, 2021, **75**(5), 1831–1840.
29 A. Yussuf, M. Al-Saleh, S. Al-Enezi and G. Abraham, Synthesis and characterization of conductive polypyrrole: the influence of the oxidants and monomer on the electrical, thermal, and morphological properties, *Int. J. Polym. Sci.*, 2018, **2018**(1), 4191747.
30 N. M. H. M. Nurazzi, S. Z. N. Demon, N. A. Halim, I. S. Mohamad, H. Bahruji and N. Abdullah, Research Progress on Polythiophene and Its Application as Chemical Sensor, *Zulfaqar. J. Def. Sci. Eng. Technol.*, 2022, **5**(1), 48–68.
31 P. Naskar, A. Maiti, P. Chakraborty, D. Kundu, B. Biswas and A. Banerjee, Chemical supercapacitors: a review focusing on metallic compounds and conducting polymers, *J. Mater. Chem. A*, 2021, **9**(4), 1970–2017.
32 L. Zhang, W. Du, A. Nautiyal, Z. Liu and X. Zhang, Recent progress on nanostructured conducting polymers and composites: synthesis, application and future aspects, *Sci. China Mater.*, 2018, **61**(3), 303–352.
33 S. Tajik, H. Beitollahi, F. G. Nejad, I. S. Shoaie, M. A. Khalilzadeh, M. S. Asl, *et al.*, Recent developments

in conducting polymers: Applications for electrochemistry, *RSC Adv.*, 2020, **10**(62), 37834–37856.
34 T. P. Kaloni, G. Schreckenbach and M. S. Freund, Band gap modulation in polythiophene and polypyrrole-based systems, *Sci. Rep.*, 2016, **6**(1), 36554.
35 M. Bajpai, R. Srivastava, R. Dhar and R. Tiwari, Review on optical and electrical properties of conducting polymers, *Indian J. Eng. Mater. Sci.*, 2016, **2016**(1), 5842763.
36 H. H. AL-Refai, A. A. Ganash and M. A. Hussein, Polythiophene and its derivatives–Based nanocomposites in electrochemical sensing: A mini review, *Mater. Today Commun.*, 2021, **26**, 101935.
37 M. G. Sumdani, M. R. Islam, A. N. A. Yahaya and S. I. Safie, Recent advancements in synthesis, properties, and applications of conductive polymers for electrochemical energy storage devices: A review, *Polym. Eng. Sci.*, 2022, **62**(2), 269–303.
38 M. N. Gueye, A. Carella, J. Faure-Vincent, R. Demadrille and J.-P. Simonato, Progress in understanding structure and transport properties of PEDOT-based materials: A critical review, *Prog. Mater. Sci.*, 2020, **108**, 100616.
39 S. Ramanavicius and A. Ramanavicius, Charge transfer and biocompatibility aspects in conducting polymer-based enzymatic biosensors and biofuel cells, *Nanomaterials*, 2021, **11**(2), 371.
40 J. Carmona-Espíndola and J. L. Gázquez, Charge transfer excitations and constrained density functional theory, *Theor. Chem. Acc.*, 2022, **141**, 1–10.
41 D. Mester and M. Kállay, Charge-transfer excitations within density functional theory: How accurate are the most recommended approaches?, *J. Chem. Theory Comput.*, 2022, **18**(3), 1646–1662.
42 A. C. Da Silva and S. I. Córdoba de Torresi, Advances in conducting, biodegradable and biocompatible copolymers for biomedical applications, *Front. Mater.*, 2019, **6**, 98.
43 G. Wang, A. Morrin, M. Li, N. Liu and X. Luo, Nanomaterial-doped conducting polymers for electrochemical sensors and biosensors, *J. Mater. Chem. B*, 2018, **6**(25), 4173–4190.
44 S. Luo, Z. Xu, F. Zhong, H. Li and L. Chen, Doping-induced charge transfer in conductive polymers, *Chin. Chem. Lett.*, 2024, **35**(1), 109014.
45 S. Iqbal and S. Ahmad, Recent development in hybrid conducting polymers: synthesis, applications and future prospects, *J. Ind. Eng. Chem.*, 2018, **60**, 53–84.
46 R. Thejas, C. Naveen, M. I. Khan, G. Prasanna, S. Reddy, M. Oreijah, *et al.*, A review on electrical and gas-sensing properties of reduced graphene oxide-metal oxide nanocomposites, *Biomass Convers. Biorefin.*, 2024, **14**(12), 12625–12635.
47 M. R. Mahmoudian, W. J. Basirun, M. Sookhakian, P. M. Woi, E. Zalnezhad, H. Hazarkhani, *et al.*, Synthesis and characterization of α-Fe2O3/polyaniline nanotube composite as electrochemical sensor for uric acid detection, *Adv. Powder Technol.*, 2019, **30**(2), 384–392.
48 D. Sun, Y. Luo, M. Debliquy and C. Zhang, Graphene-enhanced metal oxide gas sensors at room temperature: A review, *Beilstein J. Nanotechnol.*, 2018, **9**(1), 2832–2844.
49 M. S. Chavali and M. P. Nikolova, Metal oxide nanoparticles and their applications in nanotechnology, *SN Appl. Sci.*, 2019, **1**(6), 607.
50 S. Meer, A. Kausar and T. Iqbal, Trends in conducting polymer and hybrids of conducting polymer/carbon nanotube: a review, *Polym.-Plast. Technol. Eng.*, 2016, **55**(13), 1416–1440.
51 A. K. Poddar, S. S. Patel and H. D. Patel, Synthesis, characterization and applications of conductive polymers: A brief review, *Polym. Adv. Technol.*, 2021, **32**(12), 4616–4641.
52 R. Kroon, D. A. Mengistie, D. Kiefer, J. Hynynen, J. D. Ryan, L. Yu, *et al.*, Thermoelectric plastics: from design to synthesis, processing and structure–property relationships, *Chem. Soc. Rev.*, 2016, **45**(22), 6147–6164.
53 A. Jo, C. Huet and H. E. Naguib, Template-assisted self-assembly of conductive polymer electrodes for ionic electroactive polymers, *Front. Bioeng. Biotechnol.*, 2020, **8**, 837.
54 S. K. Chondath and M. M. Menamparambath, Interface-assisted synthesis: a gateway to effective nanostructure tuning of conducting polymers, *Nanoscale Adv.*, 2021, **3**(4), 918–941.
55 N. Shahzad, R. Ajmal and A. Afzal, Non-Enzymatic Electrochemical Sensors for Accurate and Accessible Uric Acid Detection, *J. Electrochem. Soc.*, 2023, **170**(9), 097505.
56 N. Y. Abu-Thabit, Chemical oxidative polymerization of polyaniline: A practical approach for preparation of smart conductive textiles, *J. Chem. Educ.*, 2016, **93**(9), 1606–1611.
57 Y. Wang, A. Liu, Y. Han and T. Li, Sensors based on conductive polymers and their composites: a review, *Polym. Int.*, 2020, **69**(1), 7–17.
58 R. Brooke, P. Cottis, P. Talemi, M. Fabretto, P. Murphy and D. Evans, Recent advances in the synthesis of conducting polymers from the vapour phase, *Prog. Mater. Sci.*, 2017, **86**, 127–146.
59 F. R. Rangel-Olivares, E. M. Arce-Estrada and R. Cabrera-Sierra, Synthesis and characterization of polyaniline-based polymer nanocomposites as anti-corrosion coatings, *Coatings*, 2021, **11**(6), 653.
60 Z. Saddique, M. Saeed and A. Afzal, Target-imprinted polyaniline/Nb_2O_5 nanoparticles as electrochemical interfaces for monitoring kidney function, *ACS Appl. Nano Mater.*, 2024, **7**(11), 13472–13480.
61 Z. S. M. Saddique, M. Faheem, S. Z. Bajwa, A. Mujahid and A. Afzal, Core–shell niobium(V) oxide@molecularly imprinted polythiophene nanoreceptors for transformative, real-time creatinine analysis, *Nanoscale Adv.*, 2024, **6**(14), 3644–3654.
62 Y. Zhang, L. Wu, W. Lei, X. Xia, M. Xia and Q. Hao, Electrochemical determination of 4-nitrophenol at polycarbazole/N-doped graphene modified glassy carbon electrode, *Electrochim. Acta*, 2014, **146**, 568–576.
63 G. Guo, Y. Sun, Q. Fu, Y. Ma, Y. Zhou, Z. Xiong, *et al.*, Sol-gel synthesis of ternary conducting polymer hydrogel for application in all-solid-state flexible supercapacitor, *Int. J. Hydrogen Energy*, 2019, **44**(12), 6103–6115.

64 T. Chen, Y. Liu, Z. Gao, Y. Gao, H. Chen, H. Ye, *et al.*, Template-assisted Flexible-to-rigid Transition of Peptides in Head-to-tail Self-polymerization Enables Sequence-controllable and Post-modifiable Peptide Nanofibers, *Angew. Chem.*, 2025, **137**(4), e202415809.

65 Y. Zhang, H. Tao, H. Wang, J. Hao, Y. Liu and Y. Yuan, Sol-gel synthesis of magnesium doped TiO2 thin film and its application in dye sensitized solar cell, *Opt. Mater.*, 2025, **158**, 116446.

66 R. R. Poolakkandy and M. M. Menamparambath, Soft-template-assisted synthesis: a promising approach for the fabrication of transition metal oxides, *Nanoscale Adv.*, 2020, **2**(11), 5015–5045.

67 M. M. Moein, A. Abdel-Rehim and M. Abdel-Rehim, Recent applications of molecularly imprinted sol-gel methodology in sample preparation, *Molecules*, 2019, **24**(16), 2889.

68 S. K. Nemani, R. K. Annavarapu, B. Mohammadian, A. Raiyan, J. Heil, M. A. Haque, *et al.*, Surface modification of polymers: methods and applications, *Adv. Mater. Interfaces*, 2018, **5**(24), 1801247.

69 W. A. K. Mahmood and M. H. Azarian, Sol-gel synthesis of polyaniline/zirconia composite conducting materials, *J. Polym. Res.*, 2016, **23**, 1–8.

70 M. M. Rahman Khan and N. Chakraborty, Conducting polymer-based gel materials: Synthesis, morphology, thermal properties, and applications in supercapacitors, *Gels*, 2024, **10**(9), 553.

71 S. Roy, S. Mishra, P. Yogi, S. K. Saxena, P. R. Sagdeo and R. Kumar, Synthesis of conducting polypyrrole-titanium oxide nanocomposite: study of structural, optical and electrical properties, *J. Inorg. Organomet. Polym. Mater.*, 2017, **27**, 257–263.

72 S. Deivanayaki, V. Ponnuswamy, R. Mariappan and P. Jayamurugan, Synthesis and characterization of polypyrrole/TiO2 composites by chemical oxidative method, *Optik*, 2013, **124**(12), 1089–1091.

73 S. M. Amorim, G. Steffen, J. M. de S Junior, C. Z. Brusamarello, A. P. Romio and M. D. Domenico, Synthesis, characterization, and application of polypyrrole/TiO2 composites in photocatalytic processes: a review, *Polym. Polym. Compos.*, 2021, **29**(7), 1055–1074.

74 J. Ji, X. Zhang, J. Liu, L. Peng, C. Chen, Z. Huang, *et al.*, Assembly of polypyrrole nanotube@ MnO2 composites with an improved electrochemical capacitance, *Mater. Sci. Eng. B*, 2015, **198**, 51–56.

75 Y. Song, Y. Dong, W. Li, Z. Tan, P. Ma, G. Wang, *et al.*, An In Situ Oxidative Polymerization Method to Synthesize Mesoporous Polypyrrole/MnO2 Composites for Supercapacitors, *Molecules*, 2024, **30**(1), 45.

76 L. Gao, C. Yin, Y. Luo and G. Duan, Facile synthesis of the composites of polyaniline and TiO2 nanoparticles using self-assembly method and their application in gas sensing, *Nanomaterials*, 2019, **9**(4), 493.

77 A. Husain, S. Ahmad and F. Mohammad, Electrical conductivity and alcohol sensing studies on polythiophene/tin oxide nanocomposites, *J. Sci. Adv. Mater. Devices*, 2020, **5**(1), 84–94.

78 A. Husain, Electrical conductivity based ammonia, methanol and acetone vapour sensing studies on newly synthesized polythiophene/molybdenum oxide nanocomposite, *J. Sci. Adv. Mater. Devices*, 2021, **6**(4), 528–537.

79 D. P. Bhattarai and B. S. Kim, NIR-triggered hyperthermal effect of polythiophene nanoparticles synthesized by surfactant-free oxidative polymerization method on colorectal carcinoma cells, *Cells*, 2020, **9**(9), 2122.

80 U. K. Aryal, N. Chakravarthi, H.-Y. Park, H. Bae, S.-H. Jin and Y.-S. Gal, Highly efficient polyacetylene–based polyelectrolytes as cathode interfacial layers for organic solar cell applications, *Org. Electron.*, 2018, **53**, 265–272.

81 Y. S. Ko and J.-H. Yim, Synergistic enhancement of electrical and mechanical properties of polypyrrole thin films by hybridization of SiO2 with vapor phase polymerization, *Polymer*, 2016, **93**, 167–173.

82 E. Pratiwi, A. Mulyasuryani and A. Sabarudin, Modification of screen printed carbon electrode (SPCE) with polypyrrole (Ppy)-SiO2 for phenol determination, *Int. Res. J. Pure Appl. Chem.*, 2018, **7**(1), 12–18.

83 A. Mane, S. T. Navale, R. C. Pawar, C. Lee and V. B. Patil, Microstructural, optical and electrical transport properties of WO3 nanoparticles coated polypyrrole hybrid nanocomposites, *Synth. Met.*, 2015, **199**, 187–195.

84 J. Sun, X. Shu, Y. Tian, Z. Tong, S. Bai, R. Luo, *et al.*, Preparation of polypyrrole@ WO3 hybrids with pn heterojunction and sensing performance to triethylamine at room temperature, *Sens. Actuators, B*, 2017, **238**, 510–517.

85 V. V. Tran, T. T. V. Nu, H.-R. Jung and M. Chang, Advanced photocatalysts based on conducting polymer/metal oxide composites for environmental applications, *Polymers*, 2021, **13**(18), 3031.

86 M. Silva, N. M. Alves and M. C. Paiva, Graphene-polymer nanocomposites for biomedical applications, *Polym. Adv. Technol.*, 2018, **29**(2), 687–700.

87 S. Ghosh, S. Das and M. E. Mosquera, Conducting polymer-based nanohybrids for fuel cell application, *Polymers*, 2020, **12**(12), 2993.

88 M. Morshed, J. Wang, M. Gao, C. Cong and Z. Wang, Polyaniline and rare earth metal oxide composition: a distinctive design approach for supercapacitor, *Electrochim. Acta*, 2021, **370**, 137714.

89 Z. Hao, M. Ruan, Z. Guo, W. Yan, X. Wu and Z. Liu, The synergistic role of the photosensitivity effect and extended space charge region in an inorganic–organic WO 3/PANI photoanode for efficient PEC water splitting, *Sustain. Energy Fuels*, 2021, **5**(11), 2893–2906.

90 T. Marimuthu, S. Mohamad and Y. Alias, Needle-like polypyrrole–NiO composite for non-enzymatic detection of glucose, *Synth. Met.*, 2015, **207**, 35–41.

91 Z. Zhang, D. Wu, L. Jiang, F. Liang, Y. Rui and B. Tang, One-step synthesis based on non-aqueous sol-gel conductive polymer-coated SnO2 nanoparticles as advanced anode materials for lithium-ion batteries, *J. Alloys Compd.*, 2022, **899**, 163274.

92 Z. Yang, C. Zhang, J. Zhang and W. Bai, Potentiometric glucose biosensor based on core–shell Fe3O4–enzyme–polypyrrole nanoparticles, *Biosens. Bioelectron.*, 2014, **51**, 268–273.

93 M. U. Khan, K. R. Reddy, T. Snguanwongchai, E. Haque and V. G. Gomes, Polymer brush synthesis on surface modified carbon nanotubes via in situ emulsion polymerization, *Colloid Polym. Sci.*, 2016, **294**, 1599–1610.

94 L. Elias, F. Fenouillot, J.-C. Majesté, P. Alcouffe and P. Cassagnau, Immiscible polymer blends stabilized with nano-silica particles: Rheology and effective interfacial tension, *Polymer*, 2008, **49**(20), 4378–4385.

95 R. D. O. Hsissou, M. Berradi, M. El Bouchti, M. Assouag and A. Elharfi, Development rheological and anti-corrosion property of epoxy polymer and its composite, *Heliyon*, 2019, **5**(11), e02789.

96 R. Hsissou, O. Dagdag, M. Berradi, M. El Bouchti, M. Assouag, A. El Bachiri, *et al.*, Investigation of structure and rheological behavior of a new epoxy polymer pentaglycidyl ether pentabisphenol A of phosphorus and of its composite with natural phosphate, *SN Appl. Sci.*, 2019, **1**, 1–9.

97 R. Hsissou, M. Berradi, M. El Bouchti, A. El Bachiri and A. El Harfi, Synthesis characterization rheological and morphological study of a new epoxy resin pentaglycidyl ether pentaphenoxy of phosphorus and their composite (PGEPPP/MDA/PN), *Polym. Bull.*, 2019, **76**, 4859–4878.

98 R. Hsissou, A. Bekhta and A. Elharfi, Synthesis and characterization of a new epoxy resin homologous of DGEBA: diglycidyl bis disulfide carbon ether of bisphenol A, *J. Chem. Technol. Metall.*, 2018, **53**(3), 414–421.

99 G. Bharath, E. Alhseinat, R. Madhu, S. M. Mugo, S. Alwasel and A. H. Harrath, Facile synthesis of Au@ α-Fe2O3@ RGO ternary nanocomposites for enhanced electrochemical sensing of caffeic acid toward biomedical applications, *J. Alloys Compd.*, 2018, **750**, 819–827.

100 C. Charan and V. K. Shahi, Cobalt ferrite (CoFe 2 O 4) nanoparticles (size:∼ 10 nm) with high surface area for selective non-enzymatic detection of uric acid with excellent sensitivity and stability, *RSC Adv.*, 2016, **6**(64), 59457–59467.

101 A. Domínguez-Aragón, A. S. Conejo-Dávila, E. A. Zaragoza-Contreras and R. B. Dominguez, Pretreated screen-printed carbon electrode and Cu nanoparticles for creatinine detection in artificial saliva, *Chemosensors*, 2023, **11**(2), 102.

102 R. J. Williams, R. D. Crapnell, N. C. Dempsey, M. Peeters and C. E. Banks, Nano-molecularly imprinted polymers for serum creatinine sensing using the heat transfer method, *Talanta Open*, 2022, **5**, 100087.

103 S. Kalasin, P. Sangnuang, P. Khownarumit, I. M. Tang and W. Surareungchai, Evidence of Cu (I) coupling with creatinine using cuprous nanoparticles encapsulated with polyacrylic acid gel-Cu (II) in facilitating the determination of advanced kidney dysfunctions, *ACS Biomater. Sci. Eng.*, 2020, **6**(2), 1247–1258.

104 J. Huang, G. Yuan, D. Cheng, F. Xie, X. Xia, X. Li, *et al.*, Sensitive electrochemical immunosensor based on MX ene-Nafion/polyaniline (PANI) for the sensitive determination of the novel biomarker sST2 for atherosclerotic coronary heart disease by differential pulse voltammetry (DPV), *Anal. Lett.*, 2024, **57**(5), 727–741.

105 T. Alizadeh and Z. Mousavi, Molecularly imprinted polymer specific to creatinine complex with copper (II) ions for voltammetric determination of creatinine, *Microchim. Acta*, 2022, **189**(10), 393.

106 S. N. Ashakirin, M. H. M. Zaid, M. A. S. M. Haniff, A. Masood and M. M. R. Wee, Sensitive electrochemical detection of creatinine based on electrodeposited molecular imprinting polymer modified screen printed carbon electrode, *Measurement*, 2023, **210**, 112502.

107 E. Saeb and K. Asadpour-Zeynali, Facile synthesis of TiO2@ PANI@ Au nanocomposite as an electrochemical sensor for determination of hydrazine, *Microchem. J.*, 2021, **160**, 105603.

108 W.-F. Hsu and T.-M. Wu, Electrochemical sensor based on conductive polyaniline coated hollow tin oxide nanoparticles and nitrogen doped graphene quantum dots for sensitively detecting dopamine, *J. Mater. Sci.: Mater. Electron.*, 2019, **30**, 8449–8456.

109 T. Xu, W. Jin, Z. Wang, H. Cheng, X. Huang, X. Guo, *et al.*, Electrospun CuO-nanoparticles-modified polycaprolactone@ polypyrrole fibers: An application to sensing glucose in saliva, *Nanomaterials*, 2018, **8**(3), 133.

110 E. B. Aydın, Highly sensitive impedimetric immunosensor for determination of interleukin 6 as a cancer biomarker by using conjugated polymer containing epoxy side groups modified disposable ITO electrode, *Talanta*, 2020, **215**, 120909.

111 R. N. Dhanawade, N. S. Pawar, M. A. Chougule, G. M. Hingangavkar, Y. M. Jadhav, T. M. Nimbalkar, *et al.*, Highly sensitive and selective PAni-CeO2 nanohybrid for detection of NH3 biomarker at room temperature, *J. Mater. Sci.: Mater. Electron.*, 2023, **34**(9), 781.

112 K.-W. Zheng, Y.-D. Zhang, Y.-S. Zhang and Y.-P. Shi, Polyaniline-Coated Flower-Like Titanium Dioxide Magnetic Fluorescent Imprinted Nanoparticles for the Determination of Transferrin in Human Serum, *Anal. Lett.*, 2024, 1–15.

113 S. Majumdar and D. Mahanta, Deposition of an ultra-thin polyaniline coating on a TiO 2 surface by vapor phase polymerization for electrochemical glucose sensing and photocatalytic degradation, *RSC Adv.*, 2020, **10**(30), 17387–17395.

114 M. Jiao, Z. Li, Y. Li, M. Cui and X. Luo, Poly (3, 4-ethylenedioxythiophene) doped with engineered carbon quantum dots for enhanced amperometric detection of nitrite, *Microchim. Acta*, 2018, **185**, 1–9.

115 S. Bukkitgar and N. Shetti, Fabrication of a TiO 2 and clay nanoparticle composite electrode as a sensor, *Anal. Methods*, 2017, **9**(30), 4387–4393.

116 G. Wang, R. Han, X. Feng, Y. Li, J. Lin and X. Luo, A glassy carbon electrode modified with poly (3, 4-

ethylenedioxythiophene) doped with nano-sized hydroxyapatite for amperometric determination of nitrite, *Microchim. Acta*, 2017, **184**, 1721–1727.

117 N. Hui, X. Sun, Z. Song, S. Niu and X. Luo, Gold nanoparticles and polyethylene glycols functionalized conducting polyaniline nanowires for ultrasensitive and low fouling immunosensing of alpha-fetoprotein, *Biosens. Bioelectron.*, 2016, **86**, 143–149.

118 W. Wang, M. Cui, Z. Song and X. Luo, An antifouling electrochemical immunosensor for carcinoembryonic antigen based on hyaluronic acid doped conducting polymer PEDOT, *RSC Adv.*, 2016, **6**(91), 88411–88416.

119 Y. Wang, C. Li, T. Wu and X. Ye, Polymerized ionic liquid functionalized graphene oxide nanosheets as a sensitive platform for bisphenol A sensing, *Carbon*, 2018, **129**, 21–28.

120 M. Li, W. Wang, Z. Chen, Z. Song and X. Luo, Electrochemical determination of paracetamol based on Au@ graphene core-shell nanoparticles doped conducting polymer PEDOT nanocomposite, *Sens. Actuators, B*, 2018, **260**, 778–785.

121 P. Bollella and L. Gorton, Enzyme based amperometric biosensors, *Curr. Opin. Electrochem.*, 2018, **10**, 157–173.

122 M. Bilgi and E. Ayranci, Development of amperometric biosensors using screen-printed carbon electrodes modified with conducting polymer and nanomaterials for the analysis of ethanol, methanol and their mixtures, *J. Electroanal. Chem.*, 2018, **823**, 588–592.

123 T. Kajisa, W. Li, T. Michinobu and T. Sakata, Well-designed dopamine-imprinted polymer interface for selective and quantitative dopamine detection among catecholamines using a potentiometric biosensor, *Biosens. Bioelectron.*, 2018, **117**, 810–817.

124 S. Jakhar and C. Pundir, Preparation, characterization and application of urease nanoparticles for construction of an improved potentiometric urea biosensor, *Biosens. Bioelectron.*, 2018, **100**, 242–250.

125 N. Kolahchi, M. Braiek, G. Ebrahimipour, S. O. Ranaei-Siadat, F. Lagarde and N. Jaffrezic-Renault, Direct detection of phenol using a new bacterial strain-based conductometric biosensor, *J. Environ. Chem. Eng.*, 2018, **6**(1), 478–484.

126 O. Soldatkina, O. Soldatkin, T. Velychko, V. Prilipko, M. Kuibida and S. Dzyadevych, Conductometric biosensor for arginine determination in pharmaceutics, *Bioelectrochemistry*, 2018, **124**, 40–46.

127 D. Minta, A. Moyseowicz, S. Gryglewicz and G. Gryglewicz, A promising electrochemical platform for dopamine and uric acid detection based on a polyaniline/iron oxide-tin oxide/reduced graphene oxide ternary composite, *Molecules*, 2020, **25**(24), 5869.

128 H. P. Singh, In-situ Generation of Au Nanostructures During Enzyme Free Oxidation of Uric Acid: A New Recognition at an Old Problem, *Colloid Interface Sci. Commun.*, 2017, **19**, 5–8.

129 J. Wang, B. Yang, J. Zhong, B. Yan, K. Zhang, C. Zhai, *et al.*, Dopamine and uric acid electrochemical sensor based on a glassy carbon electrode modified with cubic Pd and reduced graphene oxide nanocomposite, *J. Colloid Interface Sci.*, 2017, **497**, 172–180.

130 S. K. Ponnaiah, P. Periakaruppan and B. Vellaichamy, New electrochemical sensor based on a silver-doped iron oxide nanocomposite coupled with polyaniline and its sensing application for picomolar-level detection of uric acid in human blood and urine samples, *J. Phys. Chem. B*, 2018, **122**(12), 3037–3046.

131 B. Bikbov, C. A. Purcell, A. S. Levey, M. Smith, A. Abdoli, M. Abebe, *et al.*, Global, regional, and national burden of chronic kidney disease, 1990–2017: a systematic analysis for the Global Burden of Disease Study 2017, *Lancet*, 2020, **395**(10225), 709–733.

132 E. F. Carney, The impact of chronic kidney disease on global health, *Nat. Rev. Nephrol.*, 2020, **16**(5), 251–252.

133 P. Cockwell and L.-A. Fisher, The global burden of chronic kidney disease, *Lancet*, 2020, **395**(10225), 662–664.

134 S. K. Singh, X. Crispin and I. V. Zozoulenko, Oxygen reduction reaction in conducting polymer PEDOT: Density functional theory study, *J. Phys. Chem. C*, 2017, **121**(22), 12270–12277.

135 S. Bais and P. K. Singh, Al3+-Responsive Ratiometric Fluorescent Sensor for Creatinine Detection: Thioflavin-T and Sulfated-β-Cyclodextrin Synergy, *ACS Appl. Bio Mater.*, 2023, **6**(10), 4146–4157.

136 I. L. A. Zaman, S. Athar, A. Mujahid and A. Afzal, Electrocatalytic $FeFe_2O_4$ embedded, spermine-imprinted polypyrrole (Fe/MIPpy) nanozymes for cancer diagnosis and prognosis, *J. Mater. Chem. B*, 2024, **12**(24), 5898–5906.

137 M. H. Lim, R. Eres and S. Vasan, Understanding loneliness in the twenty-first century: an update on correlates, risk factors, and potential solutions, *Soc. Psychiatr. Psychiatr. Epidemiol.*, 2020, **55**, 793–810.

138 R. Salehidoost, A. Mansouri, M. Amini, S. Aminorroaya Yamini and A. Aminorroaya, Diabetes and all-cause mortality, a 18-year follow-up study, *Sci. Rep.*, 2020, **10**(1), 3183.

139 D. Liu, Y. Cheng, Z. Tang, J. Chen, Y. Xia, C. Xu, *et al.*, Potential mechanisms of methylglyoxal-induced human embryonic kidney cells damage: Regulation of oxidative stress, DNA damage, and apoptosis, *Chem. Biodiversity*, 2022, **19**(2), e202100829.

140 A. Salek-Maghsoudi, F. Vakhshiteh, R. Torabi, S. Hassani, M. R. Ganjali, P. Norouzi, *et al.*, Recent advances in biosensor technology in assessment of early diabetes biomarkers, *Biosens. Bioelectron.*, 2018, **99**, 122–135.

141 C. Karaman, O. Karaman, N. Atar and M. L. Yola, A molecularly imprinted electrochemical biosensor based on hierarchical Ti2Nb10O29 (TNO) for glucose detection, *Microchim. Acta*, 2022, **189**(1), 24.

142 J. Libich, J. Máca, J. Vondrák, O. Čech and M. Sedlaříková, Supercapacitors: Properties and applications, *J. Energy Storage*, 2018, **17**, 224–227.

143 S. Banerjee, B. De, P. Sinha, J. Cherusseri and K. K. Kar, Applications of supercapacitors, *Handbook of Nanocomposite Supercapacitor Materials I: Characteristics*, 2020, pp. 341–350.

144 G. A. Tafete, M. K. Abera and G. Thothadri, Review on nanocellulose-based materials for supercapacitors applications, *J. Energy Storage*, 2022, **48**, 103938.
145 S. Natarajan, M. Ulaganathan and V. Aravindan, Building next-generation supercapacitors with battery type $Ni(OH)_2$, *J. Mater. Chem. A*, 2021, **9**(28), 15542–15585.
146 N. R. Chodankar, H. D. Pham, A. K. Nanjundan, J. F. Fernando, K. Jayaramulu, D. Golberg, *et al.*, True meaning of pseudocapacitors and their performance metrics: asymmetric versus hybrid supercapacitors, *Small*, 2020, **16**(37), 2002806.
147 A. Tundwal, H. Kumar, B. J. Binoj, R. Sharma, G. Kumar, R. Kumari, *et al.*, Developments in conducting polymer-, metal oxide-, and carbon nanotube-based composite electrode materials for supercapacitors: a review, *RSC Adv.*, 2024, **14**(14), 9406–9439.
148 P. Sharma and V. Kumar, Current technology of supercapacitors: A review, *J. Electron. Mater.*, 2020, **49**(6), 3520–3532.
149 D. Zhao, M. Dai, Y. Zhao, H. Liu, Y. Liu and X. Wu, Improving electrocatalytic activities of FeCo2O4@ FeCo2S4@ PPy electrodes by surface/interface regulation, *Nano Energy*, 2020, **72**, 104715.
150 A. Muzaffar, M. B. Ahamed, K. Deshmukh and J. Thirumalai, A review on recent advances in hybrid supercapacitors: Design, fabrication and applications, *Renew. Sustain. Energy Rev.*, 2019, **101**, 123–145.
151 N. Wu, X. Bai, D. Pan, B. Dong, R. Wei, N. Naik, *et al.*, Recent advances of asymmetric supercapacitors, *Adv. Mater. Interfaces*, 2021, **8**(1), 2001710.
152 M. Yanilmaz, M. Dirican, A. M. Asiri and X. Zhang, Flexible polyaniline-carbon nanofiber supercapacitor electrodes, *J. Energy Storage*, 2019, **24**, 100766.
153 B. Devadas and T. Imae, Effect of carbon dots on conducting polymers for energy storage applications, *ACS Sustain. Chem. Eng.*, 2018, **6**(1), 127–134.
154 C. L. S. E. Yan, Mo Doped Nickel Sulfide with Enhanced Electrochemical Activity for Hybrid Supercapacitors, *ECS Meeting Abstracts*, 2023, (3), 809.
155 Y. Liang, D. Zhu, S. Chao, M. Hu, D. Li, W. Zhou, *et al.*, Oxygen-vacancy europium-doped MnO2 ultrathin nanosheets used as asymmetric supercapacitors, *J. Energy Storage*, 2023, **60**, 106673.
156 H. Ding, A. M. Hussein, I. Ahmad, R. Latef, J. K. Abbas, A. T. Abd Ali, *et al.*, Conducting polymers in industry: A comprehensive review on the characterization, synthesis and application, *Alex. Eng. J.*, 2024, **88**, 253–267.
157 F. Kazemi, S. M. Naghib, Y. Zare and K. Y. Rhee, Biosensing applications of polyaniline (PANI)-based nanocomposites: A review, *Polym. Rev.*, 2021, **61**(3), 553–597.
158 A. Popov, R. Aukstakojyte, J. Gaidukevic, V. Lisyte, A. Kausaite-Minkstimiene, J. Barkauskas, *et al.*, Reduced graphene oxide and polyaniline nanofibers nanocomposite for the development of an amperometric glucose biosensor, *Sensors*, 2021, **21**(3), 948.
159 Y. Zhang, J. Zhang, Y. Jiang, Z. Duan, B. Liu, Q. Zhao, *et al.*, Ultrasensitive flexible NH3 gas sensor based on polyaniline/SrGe4O9 nanocomposite with ppt-level detection ability at room temperature, *Sens. Actuators, B*, 2020, **319**, 128293.
160 D. Xing, P. Zhou, Y. Liu, Z. Wang, P. Wang, Z. Zheng, *et al.*, Atomically dispersed cobalt-based species anchored on polythiophene as an efficient electrocatalyst for oxygen evolution reaction, *Appl. Surf. Sci.*, 2021, **545**, 148943.
161 Y. A. Anisimov, R. W. Evitts, D. E. Cree and L. D. Wilson, Polyaniline/biopolymer composite systems for humidity sensor applications: A review, *Polymers*, 2021, **13**(16), 2722.
162 M. Turemis, D. Zappi, M. T. Giardi, G. Basile, A. Ramanaviciene, A. Kapralovs, *et al.*, ZnO/polyaniline composite based photoluminescence sensor for the determination of acetic acid vapor, *Talanta*, 2020, **211**, 120658.
163 C. Zuo, Y. Xiao, X. Pan, F. Xiong, W. Zhang, J. Long, *et al.*, Organic-Inorganic Superlattices of Vanadium Oxide@ Polyaniline for High-Performance Magnesium-Ion Batteries, *ChemSusChem*, 2021, **14**(9), 2093–2099.
164 A. Alipour, M. Mansour Lakouraj and H. Tashakkorian, Study of the effect of band gap and photoluminescence on biological properties of polyaniline/CdS QD nanocomposites based on natural polymer, *Sci. Rep.*, 2021, **11**(1), 1913.
165 H. J. N. P. D. Mello, M. C. Faleiros and M. Mulato, Electrochemically activated polyaniline based ambipolar organic electrochemical transistor, *Electrochem. Sci. Adv.*, 2022, **2**(6), e2100176.
166 S. Goswami, S. Nandy, E. Fortunato and R. Martins, Polyaniline and its composites engineering: A class of multifunctional smart energy materials, *J. Solid State Chem.*, 2023, **317**, 123679.
167 A. Rayar, S. Chapi, M. G. Murugendrappa, G. Babaladimath, K. Harish, R. R. Kakarla, *et al.*, Organic conjugated polymers and their nanostructured composites: Synthesis methodologies and electrochemical applications, *Nano-Struct. Nano-Objects*, 2024, **37**, 101102.
168 P. A. Thejas, R. R. Mohan, V. M. and S. J. Varma, Progress in Conducting Polymer-Based Electrospun fibers for Supercapacitor Applications: A Review, *ChemistrySelect*, 2023, **8**(17), e202203564.
169 X.-B. Zhong, H.-Y. Wang, Z.-Z. Yang, B. Jin and Q.-C. Jiang, Facile synthesis of mesoporous ZnCo2O4 coated with polypyrrole as an anode material for lithium-ion batteries, *J. Power Sources*, 2015, **296**, 298–304.
170 A. Gupta, S. Sardana, J. Dalal, S. Lather, A. S. Maan, R. Tripathi, *et al.*, Nanostructured polyaniline/graphene/ Fe2O3 composites hydrogel as a high-performance flexible supercapacitor electrode material, *ACS Appl. Energy Mater.*, 2020, **3**(7), 6434–6446.
171 S. Wang, S. Huang, M. Yao, Y. Zhang and Z. Niu, Engineering active sites of polyaniline for AlCl2+ storage in an aluminum-ion battery, *Angew. Chem., Int. Ed.*, 2020, **59**(29), 11800–11807.
172 P.-Y. Tang, L.-J. Han, A. Genç, Y.-M. He, X. Zhang, L. Zhang, *et al.*, Synergistic effects in 3D honeycomb-like hematite nanoflakes/branched polypyrrole nanoleaves

heterostructures as high-performance negative electrodes for asymmetric supercapacitors, *Nano Energy*, 2016, **22**, 189–201.

173 C. Yang, L. Zhang, N. Hu, Z. Yang, H. Wei and Y. Zhang, Reduced graphene oxide/polypyrrole nanotube papers for flexible all-solid-state supercapacitors with excellent rate capability and high energy density, *J. Power Sources*, 2016, **302**, 39–45.

174 Z. Yin, W. Fan, Y. Ding, J. Li, L. Guan and Q. Zheng, Shell structure control of PPy-modified CuO composite nanoleaves for lithium batteries with improved cyclic performance, *ACS Sustain. Chem. Eng.*, 2015, **3**(3), 507–517.

175 C. Zhou, Y. Zhang, Y. Li and J. Liu, Construction of high-capacitance 3D CoO@ polypyrrole nanowire array electrode for aqueous asymmetric supercapacitor, *Nano Lett.*, 2013, **13**(5), 2078–2085.

176 H. Zhou, G. Han, Y. Xiao, Y. Chang and H.-J. Zhai, Facile preparation of polypyrrole/graphene oxide nanocomposites with large areal capacitance using electrochemical codeposition for supercapacitors, *J. Power Sources*, 2014, **263**, 259–267.

177 I. Zykova, N. Maksimuk, M. Rebezov, E. Kuznetsova, M. Derkho, T. Sereda, *et al.*, Interaction between heavy metals and microorganisms during wastewater treatment by activated sludge, *J. Eng. Appl. Sci.*, 2019, **14**(11), 2139–2145.

178 S. Nejati, T. E. Minford, Y. Y. Smolin and K. K. Lau, Enhanced charge storage of ultrathin polythiophene films within porous nanostructures, *ACS Nano*, 2014, **8**(6), 5413–5422.

179 N. Parveen, M. O. Ansari and M. H. Cho, Route to high surface area, mesoporosity of polyaniline–titanium dioxide nanocomposites via one pot synthesis for energy storage applications, *Ind. Eng. Chem. Res.*, 2016, **55**(1), 116–124.

180 C. Arbizzani, G. Gabrielli and M. Mastragostino, Polyaniline: A new material for supercapacitor electrodes, *Electrochim. Acta*, 2001, **46**(14), 2183–2187.

181 S. Goswami, A. dos Santos, S. Nandy, R. Igreja, P. Barquinha, R. Martins, *et al.*, Human-motion interactive energy harvester based on polyaniline functionalized textile fibers following metal/polymer mechano-responsive charge transfer mechanism, *Nano Energy*, 2019, **60**, 794–801.

182 L. Gao, L. Xiong, D. Xu, J. Cai, L. Huang, J. Zhou, *et al.*, Distinctive construction of chitin-derived hierarchically porous carbon microspheres/polyaniline for high-rate supercapacitors, *ACS Appl. Mater. Interfaces*, 2018, **10**(34), 28918–28927.

183 M. A. Bavio, G. G. Acosta and T. Kessler, Polyaniline and polyaniline-carbon black nanostructures as electrochemical capacitor electrode materials, *Int. J. Hydrogen Energy*, 2014, **39**(16), 8582–8589.

184 G. Ferreira, S. Goswami, S. Nandy, L. Pereira, R. Martins and E. Fortunato, Touch-Interactive Flexible Sustainable Energy Harvester and Self-Powered Smart Card, *Adv. Funct. Mater.*, 2020, **30**(5), 1908994.

185 B. Prasanna, D. Avadhani, V. Raj, K. Y. Kumar and M. Raghu, Fabrication of PANI/SnO 2 Hybrid Nanocomposites via Interfacial Polymerization for High Performance Supercapacitors Applications, *Surf. Eng. Appl. Electrochem.*, 2019, **55**, 463–471.

186 J. Tian, N. Cui, P. Chen, K. Guo and X. Chen, High-performance wearable supercapacitors based on PANI/N-CNT@ CNT fiber with a designed hierarchical core-sheath structure, *J. Mater. Chem. A*, 2021, **9**(36), 20635–20644.

187 C. Gong, F. Deng, C.-P. Tsui, Z. Xue, Y. S. Ye, C.-Y. Tang, *et al.*, PANI–PEG copolymer modified LiFePO 4 as a cathode material for high-performance lithium ion batteries, *J. Mater. Chem. A*, 2014, **2**(45), 19315–19323.

188 C. Ajpi, N. Leiva, M. Vargas, A. Lundblad, G. Lindbergh and S. Cabrera, Synthesis and characterization of LiFePO4–PANI hybrid material as cathode for lithium-ion batteries, *Materials*, 2020, **13**(12), 2834.

189 A. B. Puthirath, B. John, C. Gouri and S. Jayalekshmi, Lithium doped polyaniline and its composites with LiFePO 4 and LiMn 2 O 4-prospective cathode active materials for environment friendly and flexible Li-ion battery applications, *RSC Adv.*, 2015, **5**(85), 69220–69228.

190 Y. Ye, P. Wang, H. Sun, Z. Tian, J. Liu and C. Liang, Structural and electrochemical evaluation of a TiO 2–graphene oxide based sandwich structure for lithium-ion battery anodes, *RSC Adv.*, 2015, **5**(56), 45038–45043.

191 C. Zhao, X. Jia, K. Shu, C. Yu, G. G. Wallace and C. Wang, Conducting polymer composites for unconventional solid-state supercapacitors, *J. Mater. Chem. A*, 2020, **8**(9), 4677–4699.

192 M. Krishna, A. Ghosh, D. Muthuraj, S. Das and S. Mitra, Electrocatalytic activity of polyaniline in magnesium–sulfur batteries, *J. Phys. Chem. Lett.*, 2022, **13**(5), 1337–1343.

193 K. Zhang, Y. Xu, Y. Lu, Y. Zhu, Y. Qian, D. Wang, *et al.*, A graphene oxide-wrapped bipyramidal sulfur@ polyaniline core–shell structure as a cathode for Li–S batteries with enhanced electrochemical performance, *J. Mater. Chem. A*, 2016, **4**(17), 6404–6410.

194 H. Guo, L. Liu, Q. Wei, H. Shu, X. Yang, Z. Yang, *et al.*, Electrochemical characterization of polyaniline–LiV3O8 nanocomposite cathode material for lithium ion batteries, *Electrochim. Acta*, 2013, **94**, 113–123.

195 L. Song, F. Tang, Z. Xiao, Z. Cao, H. Zhu and A. Li, Enhanced electrochemical properties of polyaniline-coated LiNi 0.8 Co 0.1 Mn 0.1 O 2 cathode material for lithium-ion batteries, *J. Electron. Mater.*, 2018, **47**, 5896–5904.

196 A. A. Ensafi, N. Ahmadi and B. Rezaei, Electrochemical preparation and characterization of a polypyrrole/nickel-cobalt hexacyanoferrate nanocomposite for supercapacitor applications, *RSC Adv.*, 2015, **5**(111), 91448–91456.

197 M. Barakzehi, M. Montazer, F. Sharif, T. Norby and A. Chatzitakis, A textile-based wearable supercapacitor using reduced graphene oxide/polypyrrole composite, *Electrochim. Acta*, 2019, **305**, 187–196.

198 A. K. Thakur, R. B. Choudhary, M. Majumder, G. Gupta and M. V. Shelke, Enhanced electrochemical performance of polypyrrole coated MoS2 nanocomposites as electrode material for supercapacitor application, *J. Electroanal. Chem.*, 2016, **782**, 278–287.

199 X. Wu, Q. Wang, W. Zhang, Y. Wang and W. Chen, Nanorod structure of Polypyrrole-covered MoO3 for supercapacitors with excellent cycling stability, *Mater. Lett.*, 2016, **182**, 121–124.

200 Z. Cai, H. Xiong, Z. Zhu, H. Huang, L. Li, Y. Huang, *et al.*, Electrochemical synthesis of graphene/polypyrrole nanotube composites for multifunctional applications, *Synth. Met.*, 2017, **227**, 100–105.

201 I. Staffell, D. Scamman, A. V. Abad, P. Balcombe, P. E. Dodds, P. Ekins, *et al.*, The role of hydrogen and fuel cells in the global energy system, *Energy Environ. Sci.*, 2019, **12**(2), 463–491.

202 F. Saleem, B. Ni, Y. Yong, L. Gu and X. Wang, Ultra-small Tetrametallic Pt-Pd-Rh-Ag Nanoframes with Tunable Behavior for Direct Formic Acid/Methanol Oxidation, *Small*, 2016, **12**(38), 5261–5268.

203 Z. Shi, W. Chu, Y. Hou, Y. Gao and N. Yang, Asymmetric supercapacitors with high energy densities, *Nanoscale*, 2019, **11**(24), 11946–11955.

204 K. Dutta, S. Das, D. Rana and P. P. Kundu, Enhancements of catalyst distribution and functioning upon utilization of conducting polymers as supporting matrices in DMFCs: a review, *Polym. Rev.*, 2015, **55**(1), 1–56.

205 E. B. Agyekum, C. Nutakor, A. M. Agwa and S. Kamel, A critical review of renewable hydrogen production methods: factors affecting their scale-up and its role in future energy generation, *Membranes*, 2022, **12**(2), 173.

206 M. Bodzek, Membrane separation techniques: removal of inorganic and organic admixtures and impurities from water environment, *Arch. Environ. Protect.*, 2019, **45**(4), 4–19.

207 B. Dou, H. Zhang, Y. Song, L. Zhao, B. Jiang, M. He, *et al.*, Hydrogen production from the thermochemical conversion of biomass: issues and challenges, *Sustain. Energy Fuels*, 2019, **3**(2), 314–342.

208 M. Khan, I. Al-Shankiti, A. Ziani and H. Idriss, Demonstration of green hydrogen production using solar energy at 28% efficiency and evaluation of its economic viability, *Sustain. Energy Fuels*, 2021, **5**(4), 1085–1094.

209 B. Moss, O. Babacan, A. Kafizas and A. Hankin, A review of inorganic photoelectrode developments and reactor scale-up challenges for solar hydrogen production, *Adv. Energy Mater.*, 2021, **11**(13), 2003286.

210 S.-G. Park, P. Rajesh, Y.-U. Sim, D. A. Jadhav, M. T. Noori, D.-H. Kim, *et al.*, Addressing scale-up challenges and enhancement in performance of hydrogen-producing microbial electrolysis cell through electrode modifications, *Energy Rep.*, 2022, **8**, 2726–2746.

211 H. Xiang, P. Ch, M. A. Nawaz, S. Chupradit, A. Fatima and M. Sadiq, Integration and economic viability of fueling the future with green hydrogen: An integration of its determinants from renewable economics, *Int. J. Hydrogen Energy*, 2021, **46**(77), 38145–38162.

212 M. Younas, S. Shafique, A. Hafeez, F. Javed and F. Rehman, An overview of hydrogen production: current status, potential, and challenges, *Fuel*, 2022, **316**, 123317.

213 T. Mikołajczyk, The impact of pollutants on catalyst performance during hydrogen evolution reaction: A brief review, *Synth. Met.*, 2023, **296**, 117379.

214 V. Kichigin and A. Shein, The kinetics of hydrogen evolution reaction accompanied by hydrogen absorption reaction with consideration of subsurface hydrogen as an adsorbed species: Polarization curve, *J. Electroanal. Chem.*, 2020, **873**, 114427.

215 J. Verma and S. Goel, Cost-effective electrocatalysts for hydrogen evolution reactions (HER): challenges and prospects, *Int. J. Hydrogen Energy*, 2022, **47**(92), 38964–38982.

216 S. Schumacher, L. Madauß, Y. Liebsch, E. B. Tetteh, S. Varhade, W. Schuhmann, *et al.*, Revealing the Heterogeneity of Large-Area MoS2 Layers in the Electrocatalytic Hydrogen Evolution Reaction, *Chemelectrochem*, 2022, **9**(17), e202200586.

217 Q. Sheng, Y. Du, Y. Dong, J. Zhao, X. Zhong and Y. Xie, The introduction of dual pyridinic N atoms into dibenzo [b, d] thiophene sulfone containing conjugated polymers for improved hydrogen evolution: Experimental and theoretical study, *Appl. Surf. Sci.*, 2022, **603**, 154425.

218 D. Çirmi, R. S. Karatekin, R. Aydın and F. Köleli, Hydrogen evolution and CO2-reduction on a non-supported polypyrrole electrode, *Synth. Met.*, 2022, **289**, 117102.

219 L. Xu, Y. Zhang, L. Feng, X. Li, Y. Cui and Q. An, Active basal plane catalytic activity via interfacial engineering for a finely tunable conducting polymer/MoS2 hydrogen evolution reaction multilayer structure, *ACS Appl. Mater. Interfaces*, 2021, **13**(1), 734–744.

220 A. Krishnan and S. M. A. Shibli, Electroactive P-Ani/core-shell/TiO2/TiO2-WO3 employed surface engineering of Ni-P electrodes for alkaline hydrogen evolution reaction, *J. Ind. Eng. Chem.*, 2020, **87**, 198–212.

221 R. Vinodh, C. Deviprasath, C. V. M. Gopi, V. G. R. Kummara, R. Atchudan, T. Ahamad, *et al.*, Novel 13X Zeolite/PANI electrocatalyst for hydrogen and oxygen evolution reaction, *Int. J. Hydrogen Energy*, 2020, **45**(53), 28337–28349.

222 A. E. P. Mendoza, C. Andronescu and A. Olean-Oliveira, Design of Conducting Polymer/Metal-based Nanocomposites as Electrocatalysts for Electrochemical Energy Conversion, *Synth. Met.*, 2024, 117662.

223 C. Torres, B. Moreno, E. Chinarro and C. de Fraga Malfatti, Nickel-polyaniline composite electrodes for hydrogen evolution reaction in alkaline media, *Int. J. Hydrogen Energy*, 2017, **42**(32), 20410–20419.

224 S. S. Jayaseelan, N. Bhuvanendran, Q. Xu and H. Su, Co3O4 nanoparticles decorated Polypyrrole/carbon nanocomposite as efficient bi-functional electrocatalyst for electrochemical water splitting, *Int. J. Hydrogen Energy*, 2020, **45**(7), 4587–4595.

225 M. G. Abd El-Moghny, H. H. Alalawy, A. M. Mohammad, A. A. Mazhar, M. S. El-Deab and B. E. El-Anadouli, Conducting polymers inducing catalysis: Enhanced formic acid electro-oxidation at a Pt/polyaniline nanocatalyst, *Int. J. Hydrogen Energy*, 2017, **42**(16), 11166–11176.

226 J. Wang, Q. Deng and Y. Wang, Tunable oxidation state of Co in CoOx@ N-doped graphene derived from PANI/Co3O4 and the enhanced oxygen reduction catalysis, *Appl. Surf. Sci.*, 2019, **465**, 665–671.

227 X. Cao, W. Yan, C. Jin, J. Tian, K. Ke and R. Yang, Surface modification of MnCo2O4 with conducting polypyrrole as a highly active bifunctional electrocatalyst for oxygen reduction and oxygen evolution reaction, *Electrochim. Acta*, 2015, **180**, 788–794.

228 A. Chinnappan, H. Bandal, S. Ramakrishna and H. Kim, Facile synthesis of polypyrrole/ionic liquid nanoparticles and use as an electrocatalyst for oxygen evolution reaction, *Chem. Eng. J.*, 2018, **335**, 215–220.

229 N. Alwadai, S. Manzoor, S. R. Ejaz, R. Y. Khosa, S. Aman, M. Al-Buriahi, *et al.*, CoFe2O4 surface modification with conducting polypyrrole: employed as a highly active electrocatalyst for oxygen evolution reaction, *J. Mater. Sci.: Mater. Electron.*, 2022, **33**(16), 13244–13254.

230 S. Farid, S. Ren, D. Tian, W. Qiu, J. Zhao, L. Zhao, *et al.*, 3D flower-like polypyrrole-derived N-doped porous carbon coupled cobalt oxide as efficient oxygen evolution electrocatalyst, *Int. J. Hydrogen Energy*, 2020, **45**(56), 31926–31941.

231 H. Mao, X. Guo, Y. Fu, Z. Cao, D. Sun, B. Wang, *et al.*, Efficiently improving oxygen evolution activity using hierarchical α-Co (OH) 2/polypyrrole/graphene oxide nanosheets, *Appl. Surf. Sci.*, 2019, **485**, 554–563.

232 L. Jia, G. Du, D. Han, Y. Wang, W. Zhao, Q. Su, *et al.*, Magnetic electrode configuration with polypyrrole-wrapped Ni/NiFe2O4 core–shell nanospheres to boost electrocatalytic water splitting, *Chem. Eng. J.*, 2023, **454**, 140278.

233 C. Xia, W. Chen, X. Wang, M. N. Hedhili, N. Wei and H. N. Alshareef, Highly stable supercapacitors with conducting polymer core-shell electrodes for energy storage applications, *Adv. Energy Mater.*, 2015, **5**(8), 1401805.

234 V. Gueskine, A. Singh, M. Vagin, X. Crispin and I. Zozoulenko, Molecular oxygen activation at a conducting polymer: electrochemical oxygen reduction reaction at PEDOT revisited, a theoretical study, *J. Phys. Chem. C*, 2020, **124**(24), 13263–13272.

235 Q. Zhou and G. Shi, Conducting polymer-based catalysts, *J. Am. Chem. Soc.*, 2016, **138**(9), 2868–2876.

236 A. D. Chowdhury, N. Agnihotri, P. Sen and A. De, Conducting CoMn2O4-PEDOT nanocomposites as catalyst in oxygen reduction reaction, *Electrochim. Acta*, 2014, **118**, 81–87.

237 F. Zeng, C. Mebrahtu, L. Liao, A. K. Beine and R. Palkovits, Stability and deactivation of OER electrocatalysts: A review, *J. Energy Chem.*, 2022, **69**, 301–329.

238 K. Gmucová, Fundamental aspects of organic conductive polymers as electrodes, *Curr. Opin. Electrochem.*, 2022, **36**, 101117.

239 L.-M. Cao, W. Q. Zaman, W. Sun and J. Yang, Anchoring of IrO_2 on one-dimensional Co_3O_4 nanorods for robust electrocatalytic water splitting in an acidic environment, *ACS Appl. Energy Mater.*, 2018, **1**(11), 6374–6380.

240 A. Q. Mugheri, M. S. Samtio, A. A. Sangah, J. H. Awan and S. A. Memon, Promoting highly dispersed Co3O4 nanoparticles onto polyethyne unraveling the catalytic mechanism with stable catalytic activity for oxygen evolution reaction: From fundamentals to applications, *Int. J. Hydrogen Energy*, 2021, **46**(71), 35261–35270.

241 S. Iftikhar, S. Aslam, H. Duran, S. Çitoğlu, K. Kirchhoff, I. Lieberwirth, *et al.*, Poly (3-hexylthiophene) stabilized ultrafine nickel oxide nanoparticles as superior electrocatalyst for oxygen evolution reaction: Catalyst design through synergistic combination of π-conjugated polymers and metal-based nanoparticles, *J. Appl. Polym. Sci.*, 2022, **139**(29), e52636.

242 J. Hussein, M. El-Banna, T. A. Razik and M. E. El-Naggar, Biocompatible zinc oxide nanocrystals stabilized via hydroxyethyl cellulose for mitigation of diabetic complications, *Int. J. Biol. Macromol.*, 2018, **107**, 748–754.

243 M. A. Johar, R. A. Afzal, A. A. Alazba and U. Manzoor, Photocatalysis and bandgap engineering using ZnO nanocomposites, *Adv. Mater. Sci. Eng.*, 2015, **2015**(1), 934587.

244 X. Wang, M. Zhang, J. Zhao, G. Huang and H. Sun, Fe3O4@ polyaniline yolk-shell micro/nanospheres as bifunctional materials for lithium storage and electromagnetic wave absorption, *Appl. Surf. Sci.*, 2018, **427**, 1054–1063.

245 R. Qin, L. Hao, Y. Liu and Y. Zhang, Polyaniline-ZnO hybrid nanocomposites with enhanced photocatalytic and electrochemical performance, *ChemistrySelect*, 2018, **3**(23), 6286–6293.

246 R. Saravanan, E. Sacari, F. Gracia, M. M. Khan, E. Mosquera and V. K. Gupta, Conducting PANI stimulated ZnO system for visible light photocatalytic degradation of coloured dyes, *J. Mol. Liq.*, 2016, **221**, 1029–1033.

247 E. Asgari, A. Esrafili, A. J. Jafari, R. R. Kalantary, H. Nourmoradi and M. Farzadkia, The comparison of ZnO/polyaniline nanocomposite under UV and visible radiations for decomposition of metronidazole: degradation rate, mechanism and mineralization, *Process Saf. Environ. Prot.*, 2019, **128**, 65–76.

248 A. Rajeswari, E. J. S. Christy and A. Pius, New insight of hybrid membrane to degrade Congo red and Reactive yellow under sunlight, *J. Photochem. Photobiol., B*, 2018, **179**, 7–17.

249 C. Anupama, A. Kaphle and N. G. Udayabhanu, Aegle marmelos assisted facile combustion synthesis of multifunctional ZnO nanoparticles: study of their photoluminescence, photo catalytic and antimicrobial activities, *J. Mater. Sci.: Mater. Electron.*, 2018, **29**, 4238–4249.

250 M. E. El-Naggar and K. Shoueir, Recent advances in polymer/metal/metal oxide hybrid nanostructures for catalytic applications: A review, *J. Environ. Chem. Eng.*, 2020, **8**(5), 104175.
251 Z. Zhang, L. Wang and C. Lee, Recent advances in artificial intelligence sensors, *Adv. Sens. Res.*, 2023, **2**(8), 2200072.
252 M. F. Ahmer, Q. Ullah and M. K. Uddin, Magnetic metal oxide assisted conducting polymer nanocomposites as eco-friendly electrode materials for supercapacitor applications: a review, *J. Polym. Eng.*, 2025, **45**(1), 1–41.
253 B. Dakshayini, K. R. Reddy, A. Mishra, N. P. Shetti, S. J. Malode, S. Basu, *et al.*, Role of conducting polymer and metal oxide-based hybrids for applications in ampereometric sensors and biosensors, *Microchem. J.*, 2019, **147**, 7–24.
254 M. Hatada, E. Wilson, M. Khanwalker, D. Probst, J. Okuda-Shimazaki and K. Sode, Current and future prospective of biosensing molecules for point-of-care sensors for diabetes biomarker, *Sens. Actuators, B*, 2022, **351**, 130914.